

A Quarter of a Century of Neuromorphic Architectures on FPGAs - an Overview

Wiktor J. Szczerek¹ and Artur Podobas²

¹szczerek@kth.se

²podobas@kth.se

^{1,2}KTH Royal Institute of Technology, Stockholm, Sweden

ABSTRACT

Neuromorphic computing is a relatively new discipline of computer science, where the principles of biological brain's computation and memory are used to create a new way of processing information, based on networks of spiking neurons. Those networks can be implemented as both analog and digital implementations, where for the latter, the Field Programmable Gate Arrays (FPGAs) are a frequent choice, due to their inherent flexibility, allowing the researchers to easily design hardware neuromorphic architecture (NMAs). Moreover, digital NMAs show good promise in simulating various spiking neural networks because of their inherent accuracy and resilience to noise, as opposed to analog implementations. This paper presents an overview of digital NMAs implemented on FPGAs, with a goal of providing useful references to various architectural design choices to the researchers interested in digital neuromorphic systems. We present a taxonomy of NMAs that highlights groups of distinct architectural features, their advantages and disadvantages and identify trends and predictions for the future of those architectures.

Keywords: neuromorphic systems, FPGA, computing architectures

1 INTRODUCTION

Computers and their performance improvement have historically relied on two pillars: Moore's law [1] and Dennard's scaling [2]. The former was formulated by Gordon Moore in the 1960s and states that the number of transistors per unit area double every 24 months, primarily due to improvements in lithography techniques. The latter was introduced by Richard Dennard, who found that as transistors grow smaller, the energy consumption reduces, resulting in constant power density. These two observations worked in tandem, allowing us to build more complex high-performing computers (Moore's law) without them consuming needlessly large amounts of energy (Dennard's scaling). Unfortunately, Dennard's scaling ended in 2004-2005 [3], and we are currently witnessing the slow-down of Moore's law [1] as well as the emergence of Dark Silicon [4] without any in-place replacement technology at hand [5]. Instead, researchers and industry are looking for alternative ways of computing in hope of continuing the trend in computer performance we have seen so far. These technologies are collectively called *post-Moore technologies* [6, 5] and include quantum computers [7], adiabatic reversible logic [8], and analog computing [9]. Two post-Moore technologies, however, are perhaps the most salient alternatives: Neuromorphic- [10] and Reconfigurable-computing [11, 12].

Introduced in the 1980s by Carver Mead, neuromorphic systems [13] are computers built to replicate – to various extent – the impressive computing capabilities of the biological brain. Initially designed to replicate brain circuitry using analog electronic components, neuromorphic systems today are implemented in different technologies, ranging from digitally synchronous (e.g., Intel Loihi [14] or IBM TrueNorth [15]), mixed analog/digital (e.g., BrainDrop [16]), fully analog (e.g. [17]), to even memristor- or photonics-based systems [18, 19]. Regardless of how they are implemented, they share two fundamental traits: **(i)** they communicate through discrete events called spikes and **(ii)** they are programmed in a non-imperative way, generally by encoding the problem to be solved through a spiking neural network (SNN) [20]. Solving a problem using a neuromorphic system, often results in a significantly more energy-efficient solution in several application domains [21] as opposed to a traditional von Neumann system [22]. A large number of functionalities of neuromorphic systems are driven by discoveries and innovation in

neuroscience (e.g., Spike-Timing Dependent Plasticity (STDP) [23], Bayesian Confidence Propagation Neural Network (BCPNN) [24], or Eligibility Propagation (E-prop) [25]), which has motivated many researchers to abandon non-reconfigurable and expensive application-specific integrated circuits (ASICs) and leverage the reconfigurable Field-Programmable Gate Arrays (FPGAs) to keep up with the fast pace of neuroscientific research. FPGAs [26] are a group of reconfigurable devices allowing for implementing a variety of digital circuits without the need for fabricating a bespoke ASIC. Initially designed to prototype ASICs prior to tape-out, nowadays the FPGAs are used in a plethora of different fields from low-volume electronics [27], through space exploration [28], to large data centers [29]. A hardware designer can program an FPGA to act as a central processing unit (CPU) [30], a Graphics Processing Unit (GPU) [31], or a neuromorphic device. FPGAs have shown a lot of promise in accelerating neuromorphic workloads, resulting in significant performance gains over CPU- and GPU-based solutions [32, 33], with examples of even outperforming ASIC-based neuromorphic systems (e.g., for brain simulation [34]).

This paper presents the outcome of a systematic review of neuromorphic hardware architectures integrated using FPGAs. We included majority of the literature on the subject starting from 1998, discarded unrelated works based on their abstract and/or topic, read a total of 129 papers in detail, which we then summarized and classified according to the extended taxonomy we propose. Furthermore, we identified and collected performance metrics across the surveyed literature and condensed this information in the form of trends and observations on the direction of development of the field. Finally, we conclude the survey with a discussion on future opportunities.

1.1 Motivation

There are many excellent surveys on neuromorphic systems and spiking neural networks (SNNs) from different perspectives, tied to hardware [10], specific devices [21] (e.g., Intel Loihi), different models [35], and more. For the prior work surveying FPGAs and SNNs [36, 37, 38], we found that they are very narrow in scope or outdated and that they do not cover a number of significant areas, including the analysis of trends and projections of where the field would be in the years to come. Hence, this survey is – to the best of our knowledge – the most complete review of neuromorphic hardware architectures on FPGAs and includes novel analysis of trends and projections that are not found in any other body of work on the field.

1.2 Method

To identify and select which publications to review in our survey, we adapted systematic and reproducible methods, which are outlined in the steps below:

1. With the help of the search experts from KTH Royal Institute of Technology library, we crafted a search string aimed at capturing all publications that might be relevant for the study, which we used to search in the Web of Science, Scopus, and IEEE Xplore databases. The search string we used was:

```
( TITLE-ABS-KEY ( "spiking model*" OR "spiking neur* model*"
OR "spiking network*" OR "Spiking Neur* Network*" OR
neuromorphic OR ( ( biological* OR realistic* ) W/3 ( "Neur*
Network*" OR "neur* model*" ) ) )
AND TITLE-ABS-KEY ( "coarse grained reconfigurable
architecture*" OR "coarse grained reconfigurable array*" OR
cgra OR fpga OR "field programmable gate array*" OR
"reconfigurable architecture*" ) )
```

2. The initial search query yielded more than 2128 results. We filtered and removed any duplicates and also pruned the results by reading all remaining abstracts and discarded publications irrelevant to the study (e.g., targeting Deep Neural Networks (DNNs), architectures based on CPUs or GPUs).
3. The remaining 129 publications were read, analyzed in detail, classified according to our proposed taxonomy (see Section 2.3) and included in the survey.

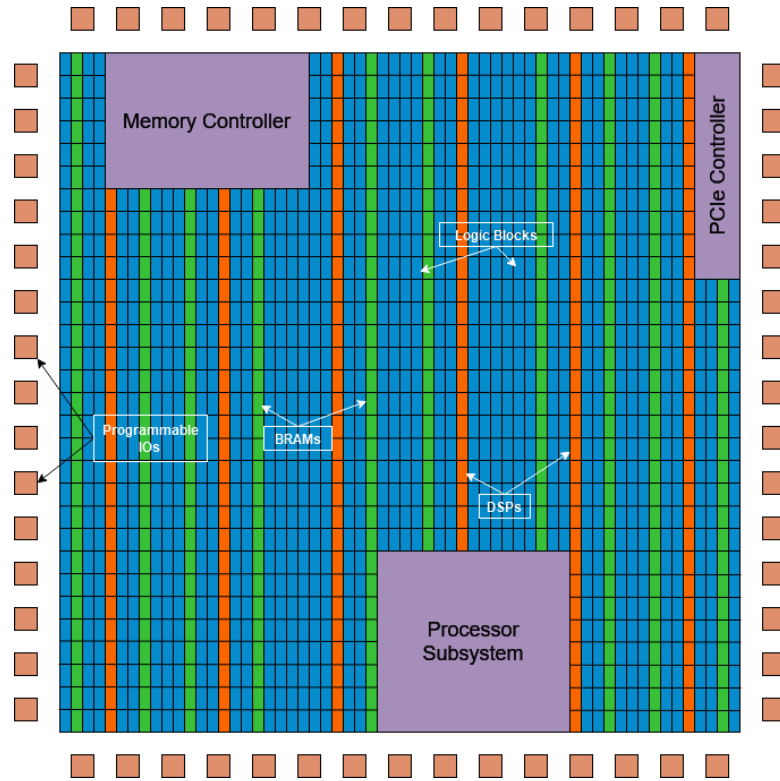


Figure 1. Abstract view of an FPGA, showing reconfigurable logic (blue), DSP-blocks (green), BRAM (red), and hardened memory controller and processor blocks. Illustration based on [12].

2 BACKGROUND

In the following section, we present the key concepts related to this survey: **(i)** the Field-Programmable Gate Arrays (FPGAs), **(ii)** Neuromorphic Architectures (NMAs) and **(iii)** Spiking Neural Networks (SNNs). Furthermore, we propose a Taxonomy for the NMAs, which we argue is necessary, considering the current lack of agreement on how to understand the term *neuromorphic hardware architecture*.

2.1 Field-Programmable Gate Arrays

Field-Programmable Gate Arrays (FPGAs)[12] belong to a family of reconfigurable architectures, whose underlying silicon can be reprogrammed to yield different functionality. Historically used to prototype ASICs before tape-out, nowadays the FPGAs are used in various different fields from low-volume electronics, through embedded systems and telecommunications to high-performance computing (HPC)[39, 40]. Performance of the FPGA-based systems can generally be better than that of the systems based on CPUs or GPUs but worse than that of custom ASICs. Another strength of using FPGAs is that they can be iteratively tailored to the needs of the application without the cost of developing a new ASIC every time. To put this matter into perspective, an FPGA capable of executing tens of billions of floating-point operations per second (tens of TFLOPs) can reach the price of thousands of dollars, while creating a similarly capable ASIC is between two and three orders of magnitude more expensive. Fundamentally, every FPGA consists of a number of *logic blocks* (also called *configurable logic blocks* or *logic elements*), a system of programmable interconnects (called *fabric*) that routes signals between the logic blocks and input/output (I/O) blocks for communication with external devices. Logic blocks are usually made up of a look-up table (LUT) that stores predefined list of logic outputs for any combination of logic input vectors and standard logic circuitry, such as multiplexers, full adders and flip-flops. The content of these LUTs can be programmed, and by connecting several LUTs together, we can achieve any digital functionality. Originally, FPGAs comprised only the aforementioned logic blocks and fabric, but it was soon realized that certain digital circuits (e.g., multipliers) consumed much of the FPGA’s logic resources. Thus, dedicated (called hardened) functionality was added to the subsequent iterations of the FPGA chips,

e.g., bespoke on-chip memory called block random access memory (BRAM), digital signal processing (DSP) blocks (which, in some FPGAs, include floating-point units) and many others (phased locked loops, PCIe controllers, etc.). Figure 1 shows a view of an FPGA.

There are multiple ways to program FPGAs. The most well-known way that also gives the best results – but also the one with the steepest learning curve – is to design logic at the register transfer level (RTL) using hardware description languages (HDLs) such as VHDL or Verilog. Another approach, which has become increasingly popular lately, is to write the intended functionality using programming languages such as C or C++ and let the compilers automatically transform the code into hardware. This is called High-Level Synthesis (HLS)[41] and allows engineers and researchers without background in electrical engineering or computer science to work with FPGAs.

2.2 Spiking Neural Networks

Biological neurons communicate via *action potentials* - voltage pulses traveling from one neuron to another, caused by rapid changes in neurons' membrane potentials - commonly referred to as *spikes* or *spike events*. Networks built using neurons that mimic this behavior are called *Spiking Neural Networks* (SNNs). SNNs are often called the *third generation networks*[20] that add a notion of time to the artificial neural networks (ANNs). SNNs have been used as tools to understand the biological brain in the neuroscience community (e.g., to study cortical columns[42]) through simulators such as Neuron[43], NEST[44], or Brian[45]. Lately, these models have also been considered for solving machine learning (ML) problems. Moreover, SNNs are believed to reduce the energy consumption needed to solve those problems and/or solve them faster, primarily by leveraging the sparseness of spike communication. Spiking neurons can be arranged in various topologies that fit different scenarios, from classification tasks to neuroscientific experiments. Those include, but are not limited to: Feed-Forward (FF) - especially the fully-connected subtype (FF-FC) which is the spiking equivalent of the multilevel perceptron (MLP), Spiking Convolutional Neural Networks (SCNNs) - which despite the feed-forward operation deserve a separate category, because of its popularity and utilization of convolutional kernels and not direct connections between neurons, Liquid State Machines (LSM)[46] - including a randomly-connected reservoir of neurons and a fully connected output layer, randomly-connected (RAND) - being a reservoir of recurrently- and randomly-connected neurons, all-to-all-connected (A2A) and biological structures represented as SNNs¹ - e.g., Central Pattern Generators (CPGs)[47, 48], which are neuronal circuits that when activated can produce rhythmic motor patterns such as walking or breathing. As for the communication, the most popular way of exchanging spike events is the Address Event Representation (AER)[49] protocol, representing the event as the destination address of a neuron or a processing element (PE) responsible for computing its dynamics, and the timestep when it occurred.

2.2.1 Neuron models

An SNN uses a *spiking neuron model* to describe the functionality of generating outgoing spikes. Those models are formulated using a set of ordinary differential equations (ODEs) that describe how a neuron cell membrane potential interacts with an injected current or modified conductance over time. In addition to the ODEs, models have a condition for emitting a spike, typically when the membrane voltage potential reaches a certain value, after which the neuron enters a state of inactivity (called *refractory period*). Neuron models vary in biological plausibility and complexity, with different models suitable for different use cases. Table 1 outlines six important neuron models, their mathematical description, biological plausibility, and an estimation of how many floating-point operations (FLOPs) are needed to advance one millisecond of simulation time using them. The Integrate-and-Fire (IF) neuron model, which is simple and biologically implausible, is also the least expensive to compute and requires only a handful of operations. On the other hand, the Nobel prize-winning Hodgkin-Huxley (HH) model is complex, describes in high detail the behavior of biological neurons, but it requires thousands of operations to solve the ODEs in a numerically stable manner. Hence, the choice of neuron model comes primarily from the use case: an SNN used for detailed simulation of the biological system might need HH-like neurons (e.g., the OpenWorm[51] project is based on these), whereas a machine learning system performing image inference might not need that level of realism, and could use a less expensive model (e.g., the Leaky Integrate-and-Fire (LIF) model, which is a popular choice for image inference[52]). While the neurons in Table 1 were selected based on them being the most popular in neuromorphic hardware (as we will see

¹Presented abbreviations are **not necessarily** used unanimously. Still, they commonly appear in the literature.

Table 1. The most commonly used spiking neuron models in our survey (see Section 4 for analysis). The biological plausibility and complexity of the model metrics are based on [50] and our own analysis. The complexity metric relates to the estimated number of floating-point operations (addition, multiplication, etc.) necessary to advance to the next timestep (1 ms) with a selected neuron model (v - membrane potential, I - synaptic current, R - leakage resistance, g_L - leakage conductance, C - membrane capacitance, g_K - conductance of the potassium ion channel, g_{Na} - conductance of the sodium ion channel; other parameters are model-specific, and interested readers are referred to the related literature for detailed explanations).

Neuron Models			
Name	Formula	Bio. plausibility	Complexity
Integrate-and-Fire (IF)	$\frac{dv}{dt} = RI$	V. Low	5 FLOPs
Leaky IF (LIF)	$\frac{dv}{dt} = -(v - V_{reset}) + RI$	Low	10 FLOPs
Izhikevich (IZH)	$\begin{cases} \frac{dv}{dt} = 0.04v^2 + 5v + 140 - u + I \\ \frac{du}{dt} = a(bv - u) \end{cases}$	Low	60 FLOPs
FitzHugh-Nagumo (FHN)	$\begin{cases} \frac{dv}{dt} = v - \frac{v^3}{3} - w + I \\ \frac{dw}{dt} = 0.08(v + 0.7 - 0.8w) \end{cases}$	Medium	100 FLOPs
Adaptive IF (AdEX)	$\begin{cases} \frac{dv}{dt} = \frac{-g_L(v - E_L) + g_L \Delta T \exp(\frac{v - v_T}{\Delta T}) - w + I}{C} \\ \frac{dw}{dt} = a(v - E_L) - w \end{cases}$	Medium	200 FLOPs
Hodgkin-Huxley (HH)	$\begin{cases} \frac{du}{dt} = \frac{-g_K n^4 (U - V_K) - g_{Na} m^3 h (U - V_{Na}) - g_{leak} (U - u_{leak}) + I}{C_m} \\ \frac{dn}{dt} = \alpha_n(U)(1 - n) - \beta_n(U)n \\ \frac{dm}{dt} = \alpha_m(U)(1 - m) - \beta_m(U)m \\ \frac{dh}{dt} = \alpha_h(U)(1 - h) - \beta_h(U)h \end{cases}$	High	1200 FLOPs

in Sections 3 and 4), there are multiple other models worth mentioning, each positioned somewhere in the span of complexity between LIF and HH[53]. These include the Spike Response Model (SRM)[54], pulsed neurons[55], Message-Based Event-Driven (MBED) neurons[56] and Traub’s model[57], to name a few.

2.2.2 Synapse Models

Neurons connect through synapses, which accept incoming spikes from other neurons. Synapses convert those spikes into a current or a change in conductance of the targeting neuron’s extensions (called *dendrites*). The current or change in conductance modifies the neuron’s membrane potential and can cause it to spike. The choice and functionality of a synapse model has a critical impact on the complexity of the hardware to a much greater extent than the choice of neuron model, mainly because there are many orders of magnitude more synapses than there are neurons[58]. Synapses, which from the biological point of view include GABA, NMDA and AMPA ion channels[59], can be modeled as current-based, where they modify the injected current into the target membrane or conductance-based (CUBA), where they modify the conductance (COBA). As with neurons, synaptic dynamics are typically described using ODEs. Synapses are extremely important and are thought to play an even larger role than neurons in an SNN. This is because synapses facilitate *learning* in the change of their *strength* (conductance). This process is called *synaptic plasticity*[60], and there are many different models available today that can be used to facilitate learning in an SNN. Most models are Hebbian[61] in nature, meaning that they relate the increase or decrease in strength to the simultaneous activity of pre- and post-synaptic neurons. One of the more popular examples is STDP[23], which modifies the strength of synapses according to how close in time a synapse induces a spike in the target neuron. Supporting plasticity in the synapse model significantly increases the computational cost of a synapse. Apart from STDP, there are other important plasticity models, e.g., Bienenstock–Cooper–Munro (BCM) rule[62] based on observations in homeostatic plasticity. There are also other methods, which can be classified as: **(i)** backpropagation-related (e.g., SpikeProp[63], Backpropagation Through Time (BPTT)[64]), **(ii)** direct-feedback-related (e-prop[25], DECOLLE[65]) and **(iii)** creating an equivalent ANN, performing learning based on Stochastic Gradient

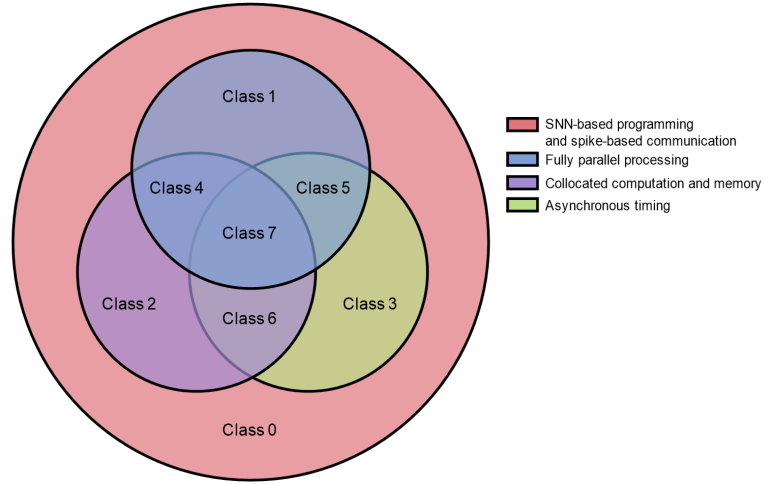


Figure 2. Proposed taxonomy - classes.

Table 2. Comparison between von Neumann architectures and NMAs according to Schuman et al. Adapted from the Figure in [66].

Property	von Neumann	Neuromorphic
Operation	Sequential processing	Massively parallel processing
Organization	Separated computation and memory	Collocated computation and memory
Programming	Code as binary instructions	Spiking Neural Network
Communication	Binary data	Spikes
Network update	Synchronous (clock-driven)	Asynchronous (event-driven)

Descent (SGD) or Backpropagation (BP) and transferring the resulting weights to an SNN.

2.3 Proposed taxonomy for Neuromorphic Architectures

Schuman et al.[66] suggest that for a system to be called *neuromorphic*, it must fulfill the following requirements: (i) it must compute using neurons and synapses (as opposed to instructions of a classical computer), (ii) it must communicate with spikes (as opposed to multi-bit values in a classical system), (iii) it is massively parallel (that is, it can compute all neurons/synapses fully in parallel), (iv) it collocates computation and memory (unlike von Neumann-based classical system), (v) it operates in an event-driven manner (the network state can be updated asynchronously, i.e., the neurons are not updated in sequence). Table 2 contrasts these properties with that of a classical (von Neumann) computer system. We propose a taxonomy for hardware neuromorphic architectures (NMAs) that builds upon that of Schuman et al., but relaxes the constraints. We argue that while a neuromorphic system must be programmed using neurons and synapses and communicate with spikes (i–ii), the remaining requirements (iii–v) are, in fact, architectural design decisions that define traits and properties of the implementation of a hardware neuromorphic architecture (NMA). To summarize, we propose that a NMA **must** perform computations using neurons and synapses and communicate with spikes, but it **may** also be massively parallel, be asynchronous, and/or co-locate computations and memory. Ultimately, this results in a taxonomy consisting of eight classes, shown in Figure 2. The latter three optional characteristics will be referred to as **Traits** for the remainder of this paper. It is important to mention that the Classes are not synonymous to grades, i.e., there are no *better* or *worse* Classes. Instead, the classification is intended to compare NMAs and implementations similar in terms of hardware and relate them to each other, like Flynn’s taxonomy [67]. Every Class comes with its own advantages and disadvantages.

3 OVERVIEW OF THE EXISTING NMAS

In this section, we present the NMAs arranged in classes as defined in the Taxonomy. As it can be seen in Figure 2, the Classes 0-3 possess at most 1 of the 3 Traits described in Section 2.3, while Classes 4-7

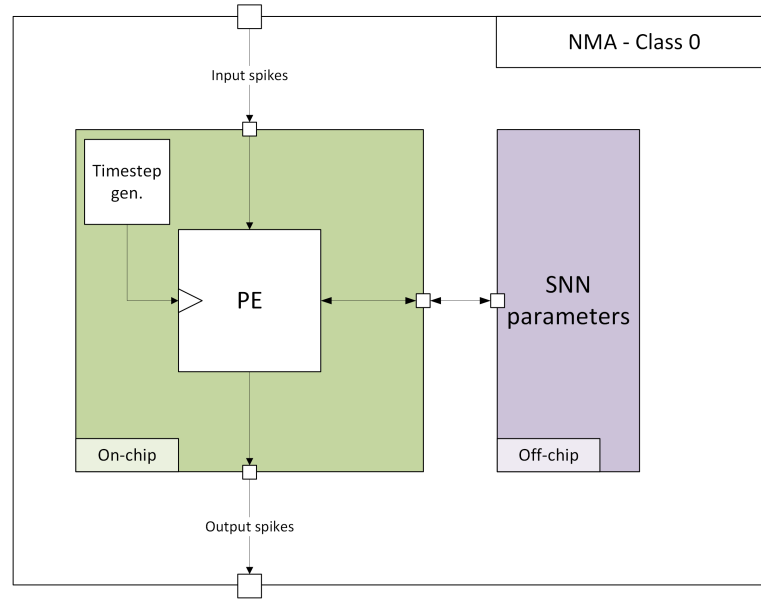


Figure 3. Simplified diagram of a Class 0 NMA.

possess 2 or all of them. Every subsection consists of a small introduction listing the features common for the appropriate Class and summaries of the surveyed architectures showing key design decisions that distinguish them from other architectures. The aforementioned subsections are divided into paragraphs for three time periods: **(i)** early implementations (1998–2009), **(ii)** early modern implementations (2010–2019) and **(iii)** modern implementations (2020–2024).

3.1 Class 0 (Traits: none)

Class 0 architectures support only SNN-based programming model and spike-based communication from the Traits listed in Section 2.3. It is common for them to include a small number of Processing Elements (PEs) that process neuron data stored in the external memory and update all neurons in sequence. Those systems have the potential of simulating the largest networks due to the arbitrary size of the attached off-chip memory, but because of that are also primarily memory-bound. They are the closest to the standard von-Neumann-like accelerators, and take the least inspiration from biology.

Early implementations. **Waldemark et al. (1998) [55]** presented a small system consisting of one neuron and two synapses, a part of a bigger network realizing a classification task. The network utilized 19% of available logic resources on Altera Flex 10K. **Jung et al. (2005) [68]** presented an NMA, where a multi-master system depends on the efficient data switch to route the data between the specific modules. They built an architecture upon the SP²INN[69] system concept and realizes a single neuron with eight fan-in connections with STDP functionality. **Glackin et al. (2005) [70, 71]** presented an architecture for realizing large-scale networks on FPGAs. They chose a LIF neuron model with dynamics approximated with Euler integration with 0.125 ms timestep. They used 18b fixed-point number representation for weights and membranes. The use case was an SNN realizing angle translation. On the Xilinx Virtex-II Pro device, the authors implemented four PEs and 400 synaptic units running at 100 MHz, resulting in 4200 neurons and 1964200 synapses achieving timestep computation time 4327 times slower than real-time. **Nuno-Maganda et al. (2009) [72]** present an NMA for recall and learning with a multi-layer FF SNN. Architecture-wise, the system comprised several arrays of PEs and Learning Modules (LMs), connected to global data and control buses via two routers. The authors tested a system with two arrays of PEs and two LMs (16 neurons) on a Xilinx Virtex-II Pro device. They chose a 16b fixed-point number representation. **Rice et al. (2009) [73]** presented an implementation of an SNN comprised of 9000 IZH neurons for character recognition in images. Architecture-wise, the system comprised several parallel pipelined time-domain multiplexed (TDM) PEs. The representation was 16b fixed-point numbers for weights and membranes. The implementation was tested with an FF-FC SNN with two layers for recognizing characters in 96x96px bitmaps and 48 classes. The system was clocked at 199 MHz on Xilinx Virtex-4

and had 25 PEs.

Early modern implementations. **Podobas et al. (2017) [32]** presented a scalable NMA relying on a single PE for neuron state update. The system supported IZH and HH dynamics, which were obtained through two approximation schemes: Euler integration with a timestep of 0.1 ms for IZH and Runge-Kutta (RK) with a timestep of 0.02 ms for HH. They used A2A networks of 14000 neurons to test the architecture on Altera Stratix-V. The synaptic connections were created from a common axon, which reduced the number of parallel computations related to spike event delivery, as well as alleviated the necessity to keep the information about the delayed spike for every connection separately. **Mostafa et al. (2017) [74]** presented an architecture for SNNs with sparse spiking activity for solving classification tasks. The architecture comprised eight PEs capable of processing 256 neurons. They chose an IF neuron model with membrane and current represented with signed 16b fixed-point number, and weights represented as signed 8b number. The implemented network had an FF-FC topology (610 neurons) and achieved an accuracy of 96.98% for the MNIST dataset. **Galindo Sanchez et al. (2017) [75]** presented a system for realizing Streaming SNN (S2NN) featuring switching off the parts of the implementation that are not needed. The design flow and the architecture assumed the implementation of FF-FC networks, layers of which could be "switched off" when not in use. The design was implemented on a Xilinx Zynq-7000 device, where the integrated ARM A9 core controlled the power management. **Kousanakis et al. (2017) [76]** presented a system with LIF neurons on a multi-FPGA system consisting of four Xilinx Virtex-6 devices. The architecture supported learning with a BCM learning rule, as well as random synaptic current generation. The system consisted of 40 PEs responsible for calculating six neurons each, with interconnectivity information and background synaptic noise stored in external memory. **Humaidi et al. (2018) [77]** compared an ANN and an SNN implementations for letter recognition on FPGA. The SNN implementation supported STDP for learning the patterns. The benchmark consisted of four different letters (5x3 pixels). The SNN was reported as more area-efficient and faster than ANN. The topology used was deduced to be a 48-neuron (IZH) WTA network.

Modern implementations. **Ahn et al. (2020) [78]** presented an architecture for realizing networks of HH neurons. The presented implementation simulated 12 million HH neurons with eight. The communication depended on the data being propagated along the axon bus from and to the PEs. The system stored duplicated information about the network state in every PE. The authors chose a neuron timestep of 0.04 ms, and the system achieved the frequency of 300 MHz on Xilinx Virtex UltraScale+. The number representation was a single-precision floating point. **Ogaki et al. (2021) [79]** presented an approach to realize HH-based SNNs with a fully dataflow-based approach². The entire system was fully pipelined. The factor differentiating this architecture from the others was an explicit focus on representing the locality of biological neuronal connections - the neurons were connected only to their neighbors in the grid (2D array topology). They showed that their architecture running a 10000-neuron system (at 300 MHz) on an Alveo U200 FPGA could be up-to 7.5x faster than a state-of-the-art CPU. **Zhou et al. (2021) [82]** presented an NMA, which relied on a set of TDM PEs capable of simulating 1024 neurons each. They utilized a weight-sharing concept, where 16 16b weights were shared throughout the synapses of the network. The architecture supported a LIF neuron model with a linear decay, instead of exponential. The system was implemented on a Xilinx Virtex-6 device and tested with the MNIST dataset with 64 PEs to realize an FF-FC network (2010 neurons), achieving an accuracy of 98.41% after 10 timesteps.

3.2 Class 1 (Traits: fully parallel)

Class 1 architectures support only fully parallel operation Trait. Those systems include number of PEs equal to the number of simulated neurons, allowing for higher speed of operation than Class 0. However, the number of neurons is bound by the amount of available logic resources on an FPGA.

Early implementations. **Maya et al. (2000) [83]** presented an architecture that comprised multiple PEs that computed a pulsed neuron - three in total - to solve the XOR problem. The weights were obtained through BP in MATLAB, and the structure was clocked at 90 MHz on Virtex VX50-6. **Xicotencatl et al. (2003) [84]** presented a network of 1120 *pulsed neurons* with 1000 synapses. The architecture was implemented on Virtex-V2000 and was clocked at 35.6 MHz. The topology of the implemented network was a 2D array of neurons.

Early modern implementations. **Moctezuma et al. (2013) [85]** presented an architecture for simulating ion-channel dynamics and membrane voltage changes of neurons defined by HH and Traub

²Using the similar platform as in [80] and [81]).

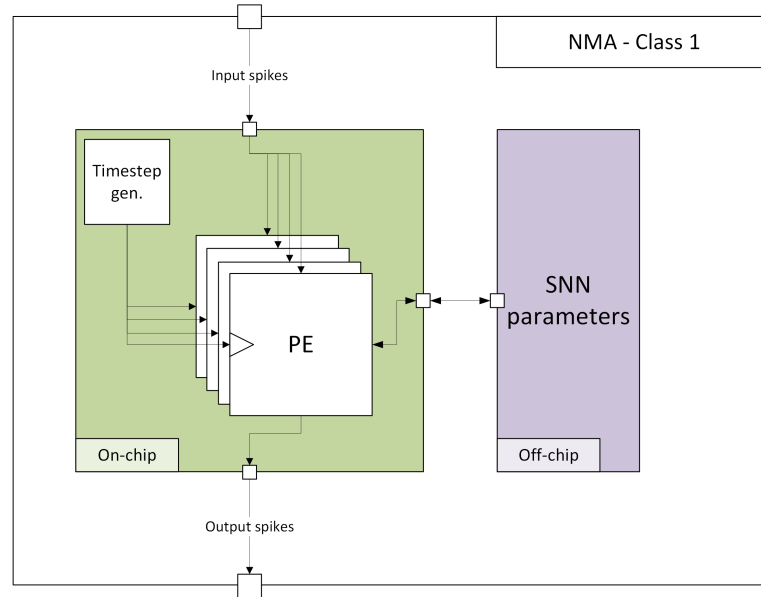


Figure 4. Simplified diagram of a Class 1 NMA.

neuron models. The models utilized floating-point arithmetic, and exponential functions were implemented as LUTs. The system was using a MicroBlaze processor for configuration and supervision, as well as communication between subunits. The entire system operated at 100 MHz and allowed the simulation of six different configurations of soma, dendrite and synapse types from the aforementioned neuron models.

3.3 Class 2 (Traits: colocated computation and memory)

Class 2 architectures support only colocated computation and memory Trait. Those architectures store network data on-chip, which limits the potential size of the implemented SNN, but allows for greater speeds of operation, in comparison to Class 0 or even Class 1, as the fully parallel operation does not bring enough benefit to balance the memory bottleneck. This class is also the most populous, as it is the easiest to implement, without the requirement for auxiliary memory support and bespoke PEs for every neuron.

Early implementations. **Schrauwen et al. (2008) [86]** presented an LSM-based recognition system for spoken digits. The system relied on serialized synapse processing and serialized arithmetic. Architecture-wise, the system consisted of a set of PEs driven by a controller block. The neuronal dynamics of an SRM model were computed in a time-multiplexed manner, but we deduced that the PEs were not pipelined. The PEs operated at 100 MHz on Xilinx Virtex-4. The authors implemented a network of 1600 neurons as a use case, to process the incoming 16 kHz audio signal with five PEs. **Thomas et al. (2009) [87]** presented an NMA using the IZH neuron model. The system allowed for simulation of 1024 neurons and 1024000 synapses, running at 100x real-time speed on a Xilinx Virtex-5 device clocked at 133 MHz. The system achieved a throughput of 2.26 GFLOPs with double-precision floating-point number representation. Architecture-wise, the system consisted of a synaptic unit, implementing four synapse pipelines, an accumulator and synaptic weight RAMs and a neuron unit with a single neuron update pipeline. **Wildie et al. (2009) [88]** presented an NMA that included a gap junction model on top of classic electrochemical synapses. They chose IZH as a neuron model for this system. Architecture-wise, the system consisted of eight PEs and could simulate a network of 1000 randomly-connected neurons. Every PE consisted of three pipelines - for neuron update, spike propagation and gap junctions dynamics. The system supported 24-bit fixed-point numerical representation for the parameters and conductance delay. It was clocked at 20 MHz and achieved 5.8x speed-up over real-time operation.

Early modern implementations. **Ambroise et al. (2013) [89]** presented an NMA that comprised 117 IZH neurons working in real-time with a 1 ms timestep. The system consisted of a single PE with separate units for neuronal and synaptic dynamics. The authors tested the implementation on a Xilinx Virtex-4 device, which was clocked at 84.809 MHz and achieved real-time operation. [90] showed a

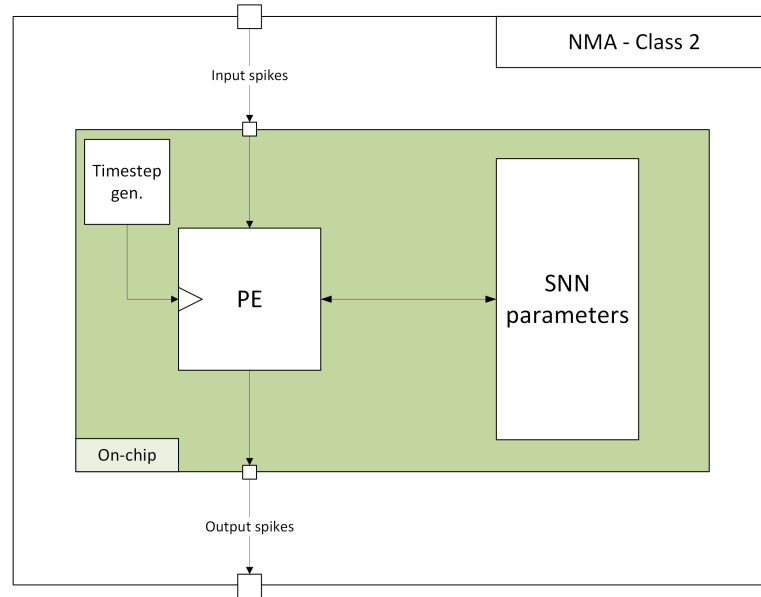


Figure 5. Simplified diagram of a Class 2 NMA.

potential use case for this architecture - implementation of a set of CPGs. **Wang et al. (2013) [91]** presented an NMA realizing a concept of a *polychronous network* (SNN where the axonal delays are used to store information instead of weights). The architecture used two arrays of PEs - one for the neurons and one for the axons - sharing two AER-based buses. The former (128 PEs) allowed for simulating 4096 neurons in biological real-time, and the latter (70 PEs) computed 1.15 million synaptic connections. The authors reported the accuracy of the memory recall to be above the 90% mark. **Yang et al. (2015) [92]** presented a system implementing a basal ganglia (BG) model. Characteristics of BG were replicated with 256 IZH neurons and 2048 synapses, and the authors claimed that the system supported up to 3k neurons on a single Altera Cyclone-IV. The implemented neuron dynamics were approximated with a 4th order piecewise-linear (PWL) approximation. The architecture consisted of four pipelines for different types of neurons found in BG and bespoke pipelines for synaptic currents. The authors chose a 28b fixed-point number representation. **Wang et al. (2015) [93]** presented a multi-FPGA architecture for implementing FF SNNs with FHN neurons. Every FPGA computed dynamics of exactly one layer and they shared a common clock signal. The devices implemented a systolic array of PEs, where every PE could compute 24 neuron dynamics within the selected timestep, and Synaptic Current Computation Modules (SCCMs) generating the presynaptic currents. **Ahn et al. (2015) [94]** presented the **Neuron Machine (NM)** - an NMA using a multi-clock domain approach, where a single soma unit operated at a higher clock rate than the synapse units. The architecture assumed a singular pipelined TDM PE per device. The authors chose a HH neuron model for their system. The memory organization relied on the concept of a *divided-and-merged* scheme, which relied on network state being cleverly duplicated for every NM in the system. The authors proved in the paper that their memory scheme allowed for lower memory utilization for up to 1000 NMs (assuming 32b floating-point representation and 10 pipeline stages) compared to a standard scheme. **Molin et al. (2015) [95]** presented a stochastic SNN-based system for performing dewarping[96] on the real-time visual data. It used an IF neuron array with random synaptic events. Those random events were sent to the accumulators responsible for specific neurons in the array (120x160 somas). The system was implemented on Xilinx Spartan-6 and was clocked at 100 MHz. **Lei et al. (2016) [97]** presented the **Efficient Neuro Architecture (ENA)** with support for approximate arithmetic, as defined in [98, 99]. They chose a two-layer WTA topology for the SNN with 800 neurons and around 640 thousand synapses for the MNIST benchmark, for which it achieved 87.7% accuracy. Architecture-wise, the system consisted of 32 PEs and supported online learning in the form of STDP. It was implemented on Virtex-6, and it was clocked at 120 MHz. **Pani et al. (2017) [100]** presented a platform for realizing real-time SNNs that could communicate with actual biological NNs (e.g., in a neuroprosthesis). The architecture relied on a varying number of TDM PEs. The presented

implementation consisted of eight PEs, each capable of realizing 180 virtual neurons and 16 synapses per neuron - implemented on Xilinx Virtex-6. The design operates at 100 MHz, and the processing was done in real-time. The authors chose the IZH neuron model with an integration timestep of 0.1 ms. **Sun et al. (2017) [101]** proposed a way of implementing an SCNN as a system to extract patterns from color-sensitive images. Architecture-wise, the system consisted of several PEs equal to the number of layers of the network. The system supported COBA LIF neurons with modifiable conductances, as well as online learning in the form of STDP. The authors used a five-layer CNN network with kernels of different sizes and types as a benchmark. **Thakur et al. (2017) [102]** presented a system for segmentation in visual processing, bringing the Integrate-and-Fire Array Transceiver (IFAT) structure[103] a VLSI CMOS array of neurons, to the FPGAs. The system is rate-encoded, utilizing Poisson spike trains for sending information from neuron to neuron. **Jailian et al. (2017) [104]** implemented Pulse Width Modulation (PWM) using SNNs. They implemented a network of IZH neurons, spiking behaviors of which were used to obtain the demanded PWM signal. Architecture-wise, there was a single IZH neuron pipeline realizing the PWM behavior, which was implemented with 6th order PWL approximation on Spartan-6. **Ambroise et al. (2017) [105]** presented a system for interfacing an SNN with a biological NN held in a Microelectrode Array (MEA). The architecture had two PEs one for the soma and one for the synaptic current. The system used IZH neurons with AMPA and GABA synapse pipelines and short-term plasticity (in Izhikievich's variant[106]). The authors tested the architecture with two CPGs with eight neurons for oscillators and four stimulation triggers with 24 inhibitory synapses. The results of the closed-loop experiments showed synchronization between the artificial and biological neurons. **Akbarzadeh-Sherbaf et al. (2018) [107]** presented a scalable architecture for randomly connected SNNs. The implemented COBA HH neurons³ were arranged in a reservoir with sparsely interconnected neurons. The architecture consisted of four PEs supporting in summary 4096 neurons on a Xilinx Artix-7 in real-time. The random generation of connections within the reservoir was performed based on a connectivity vector for one neuron (permutation-based). The neuron implementation used a 6th order PWL approximation, a 33b fixed-point representation (Q9.24) and a 1/128 ms timestep. **Sripad et al. (2018) [108]** presented SNAVA - an NMA that simulated biologically plausible SNNs on multi-device (up to 127) systems arranged in a ring topology. Every FPGA held a systolic array of PEs, connectivity units, and a router. The system supported FF networks, with one FPGA dedicated per layer. A central host controlling the simulation was connected to all FPGAs. The architecture supported IZH and LIF neuron models, as well as the STDP for online learning. The authors chose a fixed-point 16b number representation, and a 200-neuron network as a test case. They implemented it on Xilinx Kintex-7 and were able to clock it at 125 MHz with 100PEs, reaching 200 synapses and 128 neurons per PE. **Zhang et al. (2019) [109]** presented an NMA arranged as a Network-on-a-Chip (NoC) with TDM PEs. It relied on four PEs realizing LIF neurons, supporting 256 virtual neurons each within specified timestep at 100 MHz. The authors chose 9b fixed-point weights with four available values. The input was encoded as a Poisson-distributed spike train with a length of 32 events. The architecture was tested with a modified MNIST image inference use case (16x16 instead of 28x28 pixels) with FF-FC topology (522 neurons and 133632 synapses), where it achieved 96.26% accuracy. **Guo et al. (2019) [110]** presented a systolic array of PEs implementing IF neurons, designed for FF-FC networks and SCNNs. The system supported arrays of 32x32 or 32x16 PEs. The authors chose the 32b fixed-point representation for the neuronal dynamics. The system was clocked at 100 MHz on Xilinx Virtex-7, and the network operated at a timestep of one millisecond. The authors tested the system with MNIST and MNIST Fashion benchmarks for FF-FC and SCNN topologies (MNIST results: FF-FC - 98.84%, SCNN - 98.98%).

Modern implementations. **Huang et al. (2020) [111]** proposed an NMA for detecting radioisotope gamma radiation. The topology was a two-layer FF network, reflected by two TDM PEs, one per layer. The neuron model was IF with a 0.001 ms timestep. The authors verified the operation of the system by checking the membrane activity of the neurons and comparing it with the equivalent implementation on a SpiNNaker[112] platform. Weights were represented with 8b fixed-point numbers, and the system was clocked at 100 MHz. **Abdoli et al. (2020) [113]** presented an NMA designed for WTA networks simulation with IZH neurons with 0.0625 ms timestep. The NMDA and GABA ion channel dynamics were modeled. The size of the network corresponded to its biological counterpart, i.e., Center-Annular-Surround network (4500 neurons). The PEs shared a shared network activity memory, called a Total

³COBA HH neuron is even more elaborate than a standard HH neuron model, due to two additional terms in the differential equations defining its dynamics.

Spike Register. The implemented system used four PEs on Xilinx Artix-7 (up to 16 PEs would fit on this device). The authors chose a 30b fixed-point number representation for the weights. **Ju et al. (2020) [33]** presented an implementation of a particular SCNN. The system comprised three units, each realizing convolutional, pooling or fully-connected layers (7 in total). The neuron model was IF with fixed uniform encoding for the spikes. The learning process relied on performing BP on the ANN counterpart of the implemented SCNN and normalizing outputs of each layer with $[0,1]$. The weights were converted from 32b floating-point to 8b fixed-point numbers and transferred to the SNN. **Guo et al. (2020) [114]** presented a pruning process concept, relying on removing neurons from SNN, which were not crucial to determine the correct output. The idea was applied to an architecture with multiple PEs and parameters being held on-chip. Spikes were generated via LFSR, and the neuron model was a LIF with COBA synapses and triplet-wise STDP. The authors presented three different strategies for pruning: (i) constant number of neurons pruned after every batch during training, (ii) constant threshold for pruning and (iii) adaptive threshold pruning, based on the activity of a network in a current batch. **Gholami et al. (2021) [115]** presented an NMA for approximating non-linear functions. The system comprised 18 IZH neurons arranged in a FF-FC topology (9x9). The architecture relied on a singular PE that computed neuronal dynamics and performed training. The input function was encoded with Inter-Spike Interval (ISI) before reaching SNN. The SNN was taught via gradient descent - the cost function was the function of error between the expected interval and produced interval - on-chip or off-chip. The authors chose the 32b fixed-point number representation, and the integration step of 0.01 ms. **Zheng et al. (2021) [116]** presented an NMA for Vote-For-All networks (VFA), where the input layer is divided into specific receptive fields, which are later fed into several locally connected clusters sensitive to a particular input in those receptive fields. The classification output is decided based on voting from those clusters. The system used a COBA LIF model with triplet-wise STDP for online learning, and number representation of 2b for weights, and 16b fixed-point numbers for membranes. The system was implemented on Xilinx Zynq Ultrascale+, was clocked at 200 MHz and achieved 90.58% accuracy in MNIST benchmark with 2304 neurons. **Aung et al. (2021) [117]** presented **DeepFire** architecture, designed for accelerating SCNNs. The transduction and convolution and fully-connected layers consisted of several PEs, which implemented the IF neuron dynamics. The test cases included MNIST and CIFAR-10 benchmarks, for which the system achieved the following results: MNIST - 99.14% at 40.1kFPS; CIFAR-10 - 81.8% at 28.3kFPS. **Wu et al. (2021) [118]** presented an NMA supporting STDP implemented using a Fast CORDIC algorithm. The architecture consisted of a 14x10 array of TDM PEs and implemented a 2-layer FF-FC for MNIST benchmark. The second layer was a WTA layer with lateral inhibition, where a sum of votes from multiple neurons was considered. The authors used a LIF neuron model. The system supported STDP without dynamic leakage for the presynaptic trace with Fast-CORDIC-based learning, which resulted in 50% reduction in the number of iterations before convergence in comparison to the standard CORDIC algorithm. The authors chose a fixed-point 8b numbers for the weights and 16b fixed-point numbers for the membranes. They implemented the system on a Xilinx Zynq-7000 device. **Ali et al. (2022) [119]** presented an implementation of an SNN intended for image inference. It was a purpose-built architecture targeting the simplified MNIST data (5x5 pixels, binary pixels, two classes), with the network topology being an FF-FC (7 neurons). The neurons were organized in layer blocks, which performed calculations for the specific neurons in a time-multiplexed fashion. The authors chose the 8b fixed-point number representation. The system was clocked at 25 MHz, and achieved 95.16% accuracy on Xilinx Artix-7 for the simplified MNIST benchmark. **Hwang et al. (2023) [120]** presented **ReplaceNet** - SW/HW co-design framework for designing SNN-based replacements of the sub-portions of biological neural networks. It supported supervised STDP to train several LIF neurons to provide accurate spike timings of their biological counterparts, dubbed SA-STL (STDP Assisted Spike Timing Learning). Architecture-wise, the system was a systolic array of PEs, each containing a LIF neuron and synaptic pipelines. The system was operating in real-time, which the authors achieved for levels of connection sparsity from 0% to 90% on Xilinx Zynq-7020. **Kauth et al. (2023) [121]** presented **neuroAIx** framework - an initiative for realizing NMAs on any cluster of processing elements (such as a system comprising 35 NetFPGA SUME boards, presented in the paper). The architecture of neuroAIx was a NoC of FPGA devices (nodes) with a centralized main router and A2A connections in the same row and column of the array. Each node consisted of 8GB of off-chip DDR3 memory and held several PEs connected in a round-robin fashion. The nodes were allowed to progress to the next timestep if neighbors within two hops completed their calculations for a current timestep. The implementation

supported LIF and IZH neurons with 32b floating-point representation for both weights and membranes. The test case presented in the paper was the cortical microcircuit[42] that achieved a 0.46% difference in spike generation over the software simulation (NEST). **Wang et al. (2023) [122]** presented an NMA for realizing a path planning algorithm using SNN based on IZH neurons. Architecture-wise, the system comprised a grid of TDM PEs (6x6), where every PE was responsible of a specific square of neurons (24x24). Those neurons directly represented the map of the environment in which objects could move in eight directions. The system used STDP for learning the path. The authors used the IZH neurons with CORDIC and Binary-based multiplier optimizations. The system operated with a 0.1 ms timestep 2000x faster than real-time on Altera Cyclone-IV clocked at 134.36 MHz. **Wang et al. (2023) [123]** focused on creating an architecture for SCNNs with module reusability. Reusability was understood as not storing the intermediate states of neurons in memory but instead reusing memory and pipelines as the features propagate through the network. The authors chose the LIF neuron model for neuronal dynamics. Two SCNNs were implemented as test cases for image inference (MNIST - 98.15% accuracy, CIFAR-10 - 85.71% accuracy). **Shi et al. (2024) [124]** presented an LSM with stateless reservoir neurons and a trainable output layer based on IF neurons. The IF neurons in the reservoir did not store the membrane potentials in memory - the potential was obtained on the fly. Architecture-wise, the system consisted of an array of reservoir computing units and readout computing units, with a controller managing both arrays' operations. The neurons communicated via AER-compliant protocol. The network was taught with a BP-STDP method. **Chen et al. (2024) [125]** presented an SCNN accelerator. The system comprised blocks responsible for either a layer computation or pushing intermediate results between layers. The implemented network had two convolutional layers that utilized STDP, one convolutional layer using supervised STDP, two pooling and two padding layers. The authors chose the IF neuron model with single-spike encoding. For the MNIST benchmark, the system achieved 95% accuracy, with a processing time of 0.16s per image inference on Xilinx Zynq Ultrascale+, clocked at 100 MHz. **Liu et al. (2024) [126]** presented an architecture relying on stochastic LIF neurons and PLR learning rule[127] to realize the synaptic plasticity. By adjusting the synaptic weights, the neuron could anticipate future inputs based on the patterns and correlations it had observed in the past. Architecture-wise, the system relied on a systolic array of 64 PEs. The authors tested the system with three use cases: robot arm, swarm collision avoidance and MNIST benchmark (90.19% accuracy on Xilinx Zynq-7000).

3.4 Class 3 (Traits: asynchronous network update)

Class 3 architectures support only the asynchronous network update Trait. Those systems have a possibility of reduced power consumption, due to updating the network state only when there are spikes generated. However, the number of neurons is bound by the amount of available logic resources on an FPGA.

Early implementations. **Hellmich et al. (2004,2005) [128, 129]** presented **SNN Emulation Engine (SEE)**, which they claimed it could support up to 50 million IF neurons and 800 million synapses. The architecture organization relied on three FPGAs responsible for: (i) network configuration, monitoring and administration, (ii) computation of the target neurons addresses and (iii) updating neuron potentials and weight updates. A set of three PEs was implemented on the third device connected to three bespoke SDRAMs. The neuron update used a Bulirsch-Stoer integration method. **Ros et al. (2006) [130]** presented **RT-Spike**, which was a SW/HW hybrid architecture for realizing SNNs with SRM-model-based neurons. The authors chose a 14b fixed-point number representation. They tested the system with a network of 1024 neurons on four PEs and achieved real-time operation on Xilinx Virtex-2000E at 25 MHz, with 4.16 million updates of the network state per second. **Glackin et al. (2009) [131]** presented **Reconfigurable Architecture**, which aimed at modeling the biological functions of the brain. The architecture comprised a set of PEs simultaneously simulating up to 250 neuron with COBA LIF and SRM neuron models support. Reconfiguring the network was performed on-the-fly, by changing the values in the BRAM memory via a custom DMA core. The implemented system performed edge detection on 512x512 px images on a Xilinx Virtex-4 device with four PEs, using an SCNN with 1.05 million neurons and 52.4 million synapses, reaching 1.05 seconds of inference time per image.

Early modern implementations. **Yang et al. (2011) [132]** presented an NMA for explaining the computational capability of the early stage of the primate visual system. The input for the topology was a gray image transformed into a temporal firing rate in a given period. The architecture used four FPGAs, one per every image orientation feature, with 64 TDM PEs per device, allowing for one million LIF neurons and two million synapses. It was implemented on the Xilinx Virtex-4 device and clocked at 200

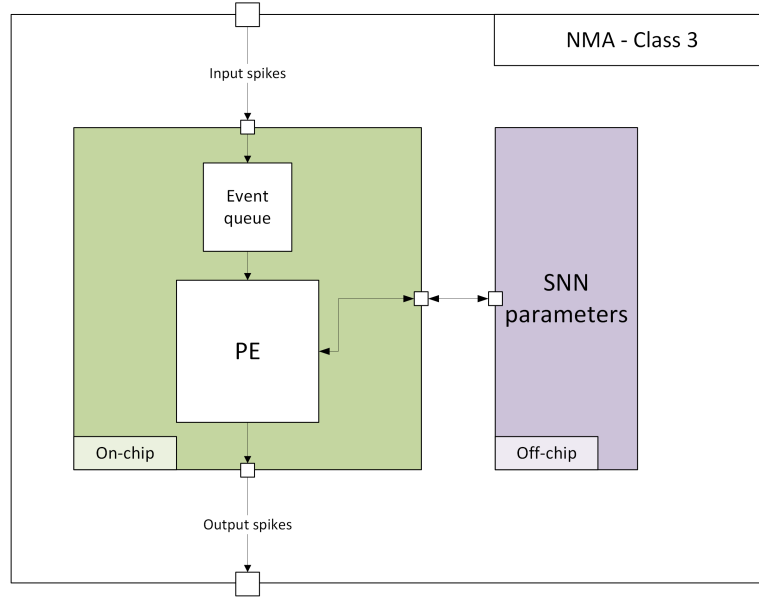


Figure 6. Simplified diagram of a Class 3 NMA.

MHz. **Neil et al. (2014) [133]** presented **Minitaur** - an SNN accelerator designed for image inference and robotics applications⁴. The architecture comprised 32 PEs with bespoke state and weight information caches. The neuron model was LIF with a decay rate based on the distance in time between the consecutive events. The system used broadcasting, instead of point-to-point connections. The authors chose a 16b fixed-point number representation for most of the parameters and values. The system implemented on Xilinx Spartan-6 device achieved 92% accuracy in MNIST benchmark, using an FF-FC network with 1010 neurons and was clocked at 75 MHz. **Cheung et al. (2016) [80]** presented **NeuroFlow** - a complete framework for implementing dataflow-based NMAs⁵. The design flow assumed that the necessary data was stored in the external memory, and processed by two sets of PEs: one for fetching the information and one for accumulating the spiking events and weights. The generated architectures supported a variety of neuron models (LIF, AdEx IF, IZH and HH), integration methods (Euler, RK4), synaptic input current kernels (exponential, alpha or custom) and a pair-based nearest neighbor STDP. The benchmarks included a simulation of 589824 neurons with varying numbers of synapses on four Xilinx Virtex-6 devices and a simple test of the STDP mechanics between two AdEx neurons. **Wang et al. (2018) [135]** presented an NMA for simulating mini- and hypercolumn models of the human neocortex. The system followed a hierarchical structure, where a network is implemented as a set of interconnected hypercolumns consisting of several minicolumns (up to 128), where every minicolumn comprised up to eight different types of heterogeneous neurons (100 per minicolumn). The neurons followed a two-compartment COBA LIF model, integrated with a 1 ms timestep. The representation of the weights and postsynaptic potentials was fixed-point 4b numbers, and the system supported axonal delay. The authors tested the system with a simulation of an auditory cortex divided into 100 channels sensitive to different sound frequencies. They mapped every channel to 100 hypercolumns, resulting in 10 thousand hypercolumns with 100 million LIF neurons. The authors claimed the maximum number of neurons and synapses supported by the architecture on an Altera Stratix-V to be 20 million and four trillion, respectively.

Modern implementations. **Han et al. (2020) [136]** presented an NMA with a single processing pipeline for LIF neuron dynamics. The authors introduced zero-biased ReLU-based offline training, as well as a hybrid updating algorithm, which, according to them, merged the event-driven and timed operation. They achieved it with separate event queues for a number of consecutive timesteps. The authors claimed the system supported 16384 neurons on Xilinx Kintex-7, and they tested it with the MNIST benchmark and FF-FC network (2058 neurons), for which it achieved an accuracy of 97.06% and was

⁴There was also the **n-Minitaur** system[134] which was heavily based on Minitaur and was an adaptation of that system to support processing of the data from up to three spike-based sensors.

⁵This idea was first presented in [81].

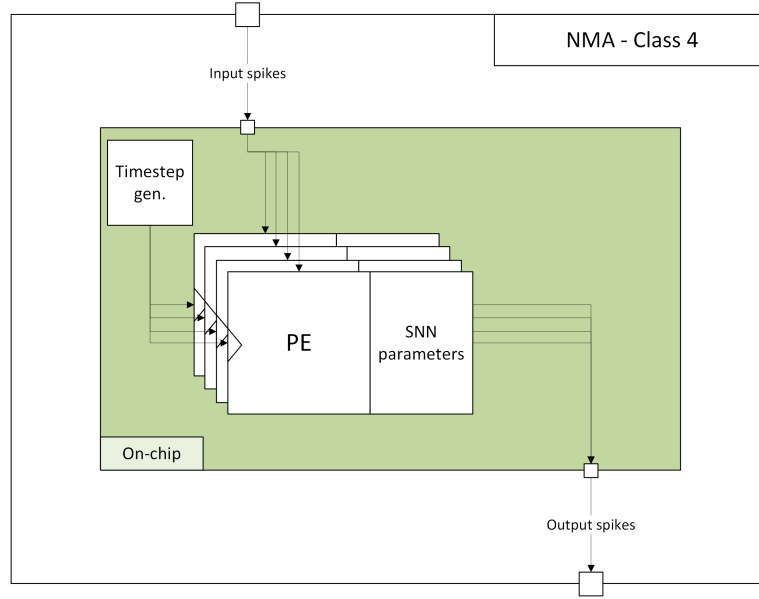


Figure 7. Simplified diagram of a Class 4 NMA.

clocked at 200 MHz, with processing speed of 161 frames per second. **Li et al. (2021) [137]** presented an NMA with a clock/event-driven hybrid update scheme - however, according to the Features described in Section 2.3, the system is a member of Class 3. It comprised 12 PEs with five computational cores (CC) in every PE, supporting CUBA LIF neurons with STDP-based learning capability. The four out of five CCs mentioned above could be shared with neighboring PEs. The architecture was implemented on Xilinx Virtex-7 and tested with the MNIST benchmark and FF-FC (310 neurons) network topology with 16b floating-point representation, achieving 85.28% and the speed of 61FPS, clocked at 100 MHz. **Liu et al. (2022) [138]** presented **FPGA-NHAP**, designed with a simulation of FF topologies in mind. From an architectural point of view, the system was a single neural core that comprised 16 PEs and supported LIF and IZH neurons via two different pipelines, which were used to process neurons in a time-multiplexed manner. The network size was bound by the 14-bit addressing to 16384 neurons and 16.77 million synapses (with an A2A topology). The connectivity was stored in memory in a form of crossbars, and its size was fixed and architecturally bound. The authors chose a 16b signed fixed-point number representation. The system achieved the accuracy of 97.7% for LIF and 97.81% for IZH for the MNIST benchmark and 85.14% for LIF and 83.16% for IZH for the Fashion MNIST benchmark. **Chen et al. (2024) [139]** presented **SiBrain** - a spatio-temporal parallel NMA targeting SCNNs. The architecture comprised 64 PEs. It achieved 99.08% accuracy for the MNIST benchmark with processing speed of 512 frames per second and 90.25% accuracy for the CIFAR-10 benchmark at 53 frames per second. The system was clocked at 200 MHz and implemented on Xilinx Virtex-7 2000T.

3.5 Class 4 (Traits: fully parallel, collocated computation and memory)

Class 4 architectures support two Traits: fully parallel operation and collocation of memory and computation. They have the potential of updating the entire network the fastest out of all of the Classes, however due to the entire system - including the event processing circuitry - being contained on-chip, they are the most dependent on the amount of available resources on the FPGA platform. *Early implementations.* **Roggen et al. (2003) [140]** presented an NMA for autonomous agents with on-the-fly reconfiguration capability. The authors chose a LIF neuron model, and the topology was a 2D array of 8x8 neurons. Architecture-wise, the system comprised 64 PEs with parameters kept on-chip, and it was clocked at 33 MHz on Altera APEX20K200E. **Bellis et al. (2004) [141]** presented an NMA, which was a hardware port of a software-based simulator. The network comprised four LIF neurons and four synapses, and its main task was to solve the wall-following task for an autonomous agent. Architecture-wise, we deduced that there were four PEs and that the system was clocked at 118.189 MHz on Xilinx Spartan-2, with a fixed-point representation of 5b width for weights and 7b for membrane potential. **Upegui et al.**

(2005) [142] presented a framework for design space exploration (DSE) for SNNs, based on the genetic algorithm approach (the authors called it the *evolutionary algorithm*). The authors used the Dynamic Partial Reconfiguration (DPR) for NMA reconfiguration. The architecture comprised a varying number of PEs and a weight adjustment units and two fixed modules - encoder and decoder for input and output. The PEs and weight adjustment units were DPR-compliant, which could consist of single neurons, layers, or entire networks. The genetic algorithm was used to find the optimal network topology. The system supported a LIF neuron model and the STDP weight-adjusting method. **Guerrero-Rivera et al. (2006) [143]** presented implementations of various logic designs for LIF neuronal dynamics with STDP and axonal delays using the Exact Integration method⁶. The authors focused on deploying parallel, low-complexity neuron model implementations without resource sharing, which operated in a single-cycle manner. The architecture supported exponential decay for the LIF neurons, and alpha and beta synaptic kernels with STDP for synapses. The authors used the system to describe two classes of neurons in the mammalian olfactory bulb and deployed it on Xilinx Virtex-II Pro, clocked at 33 MHz. **Shayani et al. (2008) [145]** presented the implementation of an SNN with Piecewise-Linear Approximation of Quadratic Integrate and Fire (PLAQIF) neurons. Their main goal was heterogeneous recurrent SNNs implementation, with support for a certain degree of structural plasticity. Architecture-wise, the system comprised 161 PEs with several synapse units per PE arranged in a column and interconnected in a daisy-chain fashion. The upstream packets (from soma) were unchanged and passed-through the synapses in the column, while downstream packets were processed by the synapse. The authors tested the implementation with a recurrent network of 161 neurons on the Xilinx Virtex-5 device clocked at 160 MHz.

Early modern implementations. **Johnston et al. (2010) [146]** presented an *evolution-based* SNN on FPGAs for robotics, designed with a HW/SW co-design methodology. They implemented the evolutionary part of the SNN a genetic algorithm, and added the STDP-based online learning for fine tuning the network obtained through genetic algorithm. The system functioned as an intelligent controller for a robotic system to solve autonomous navigation and obstacle avoidance. Architecture-wise, it relied on the network unit and embedded microcontroller to perform the update through the genetic algorithm. The authors tested the system on a Khepera robot[147] with 10 LIF neurons and 16 synapses. The implementation was clocked at 100 MHz on a Xilinx Virtex-II Pro and used 16b floating-point arithmetic. **Caron et al. (2011) [148]** presented an implementation of the Hierarchical SNN (HSNN) based on the Oscillatory Dynamic Link Matcher (ODLM) algorithm, i.e., using LIF neurons to approximate the behavior of relaxation oscillators. They claimed that just like ODLM, the HSNN could perform image segmentation, matching, and monophonic sound source separation. Architecture-wise, the system comprised an HSNN unit, controller and communication units. The HSNN used a bit slice architecture composed of several columns connected in a ring buffer. Said slices were built off of a weight memory containing all of the presynaptic weights to the neuron instantiated by the column, and the synapse model unit, which added the synaptic weights to the neurons' potential during spike propagation. **Rossello et al. (2012) [149]** presented an NMA for stochastic SNNs. The architecture used a non-standard IF neuron model - the authors used a shift register where the single bit was being shifted depending on the signal from the synapses. The incoming spikes were only passed to the shifting logic if matched with the partial probabilities, realizing the stochastic operation. When the bit reached the MSB position, the spike was propagated further. The authors tested the system with a high-speed signal filtering and solving complex systems of linear equations tasks on Altera Cyclone-III, with a single layer of 100 output neurons. **Iakymchuk et al. (2012) [150]** proposed an NMA that efficiently implemented large networks on low-end hardware. The architecture supported a one millisecond biological timestep and featured a set of PEs that serially processed the input. The authors chose the SRM model for synapses and neurons and divided the system into three primary levels: neuron, layer, and network, which were realized by units consisting of a set of subunits from lower levels of the hierarchy. They utilized spike encoding with a specified frequency of spike trains, and chose 16b fixed-point arithmetic, with weights being drawn from a set of 30 16b fixed-point values. They tested the system on a Xilinx Spartan-3, with a pattern classification on 3x3-bit arrays using FF-FC network (9x9x4). **Deng et al. (2014) [151]** presented an NMA for a specific topology of an FF-FC network to achieve synchronization in neuron spiking between the layers, starting from uncorrelated firing rates. The architecture assumed using bespoke PEs per synapse and neuron. The authors chose the LIF neuron model and alpha kernel for the synaptic dynamics. The system achieved the intended synchronized firing between the layers on the Altera Stratix III clocked

⁶The authors thoroughly described it in another work [144].

at 50 MHz, with an 8x8x8 network, achieving 50000x real-time operation. **Wang et al. (2015) [152]** presented a general-purpose Liquid State Machine (LSM) network with a reconfigurable reservoir of randomly connected LIF neurons and pre-trained, task-specific fully-connected output layers. The authors implemented the reconfigurability of the reservoir's neurons via power gating (turning off the unused parts of the FPGA). The plasticity was implemented with probabilistic weight updates and an induced teaching signal. The architecture relied on a set of PEs realizing the liquid neurons making up a *reconfigurable unit* and a set of PEs making up a *trainable unit* for the output functionality. The implementation presented in the paper used 135 liquid neurons (which can be sized down to 90), and 26 output neurons on a Xilinx Virtex-6. The number of output neurons depended on the output of the most demanding task the system was designed to perform. The accuracy for the MNIST benchmark was 98.6% for the largest available network (135 reservoir neurons and 26 output neurons). **Farsa et al. (2015) [153]** presented an NMA for a single layer SNN performing function approximation. In a sense, it was a generalized classification task, as function computation was replaced by classifying input into various coded outputs. The authors chose the LIF neuron model for the system. The learning part was performed with MATLAB and SGD, which resulted in a set of weights that could be mapped to a single-layer WTA network. From the architectural point of view, the entire system comprised several PEs responsible for their bespoke neurons. The system was used to approximate the Gaussian force field as a test case and implemented on a Xilinx Zynq-7000. **Gomar et al. (2016) [154]** presented an implementation of a neuron-synapse-neuron connection with additional astrocyte block connected to both neurons. Their main goal was to implement an astrocyte along the neurons efficiently. The authors employed an AdEx neuron model, the Kopel model for synapse and the Postnov model for astrocyte dynamics, resulting in six ODEs. As for the models, the authors optimized them by approximating the costly functions in the ODEs - *exp* and *tanh* - with Base-2 term and sign function, respectively. With the latter, the authors showed that Base-2 could also be used, but the sign was significantly cheaper implementation-wise. The implementation was tested on Xilinx Virtex-II. **Lammie et al. (2018) [155]** did not focus on a specific architecture but rather on presenting an optimization approach for a specific NMA. The authors presented a way of utilizing a single vector of IZH neurons, arranged in a WTA topology with lateral inhibition, to recognize patterns after training them with STDP. The design was rate-based, and the spikes were Poissonian. The IZH neurons used bit shifts and adders to reduce the computational cost of multipliers. The STDP mechanism was simplified, where instead of holding the approximate values, it was approximated directly in circuitry via combination of OR gates. **Heidarpur et al. (2019) [156]** presented a coordinate rotation digital computer (CORDIC)-based SNN based on IZH neurons. Despite the fact that the paper focused on the optimizations applied to the neuron computing pipeline rather than on the actual architecture choices, the authors suggested how to use this concept paired with STDP, which showed potential on how to create a larger NMA. The implemented network comprised 21 neurons, but the authors claimed they could potentially fit 110 neurons on a Xilinx Spartan-6 clocked at 183.4 MHz. **Kuang et al. (2019) [157]** presented an NMA for realizing a specific SNN. The topology comprised three layers of neurons equal to the resolution of the input image. The operation assumed the output layer being made out of excitatory neurons, and the output is the firing pattern of this layer. The neurons were LIF with COBA synapses with exponential leakage and support for triplet-based STDP. The system was pipelined to increase the throughput. The authors tested the implementation with a simplified MNIST benchmark (5x5 instead of 28x28 pixels) for a network of 75 neurons that achieved 93% accuracy.

Modern implementations. **Asgari et al. (2020) [158]** presented an NMA for an SNN comprising an input layer and two layers of WTA networks, for simulating a simplified model of hippocampal and motor neurons. The architecture comprised an array of PEs for neurons and synapses, a crossbar for connection and activity memory, and a designated activity block for the WTA mechanic. The authors chose a LIF neuron model and the synapses were fixed in weight for the inhibitory and followed the STDP learning rule for the excitatory type. The STDP was implemented as a LUT for 16 time intervals and 10 possible weight modification values. **Liang et al. (2021) [159]** proposed an SNN accelerator targeting image inference. The network model used a single-spike encoding scheme, where the neurons fire exactly once per inference. Architecture-wise, the system was a systolic array of eight PEs, where every core comprised an 8x8 array of neurons and a shared weight memory. The PEs were connected in a bidirectional list organized in two columns of four PEs. The architecture was tailored for a specific use case and a specific network topology, i.e., FF-FC (522 neurons). **Deng et al. (2021) [160]** presented an implementation of an auditory NN. The system comprised six layers of 11 LIF neurons. The input

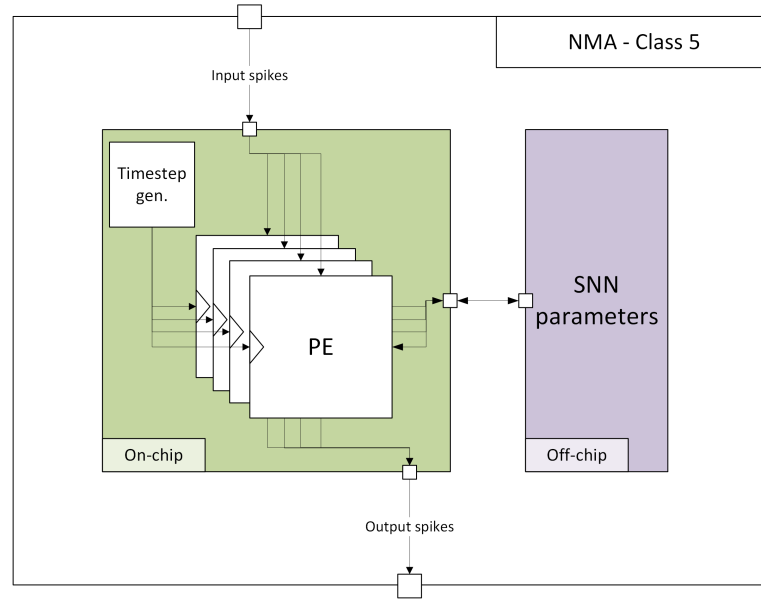


Figure 8. Simplified diagram of a Class 5 NMA.

auditory data were passed through the layers, and the results from all the layers were transferred to the centralised Bayesian classifier module. The synapses realized the spike traces with exponential kernels. The design was multiplierless, utilizing bit shifts and adders. The authors conducted tests on the system with speech samples consisting of spoken digits with applied noise (from 20dB to -5dB signal-to-noise ratio). According to the authors, the results suggested that this implementation was somewhat resilient to noise, reaching around 50% accuracy with -5dB SNR. **Heitmann et al. (2022) [161]** used **IBM's INC-3000 Neural Supercomputer** - a massive neural simulation system that comprised 16 boards, each including 27 Xilinx Zynq-7045s (called nodes) to implement the cortical microcircuit[42]. The architecture was a hierarchical NoC where every board implemented a cube of 3x3x3 of nodes. Those cubes were connected in a 4x4 array. This connection scheme resulted in a grid of 12x12x3 (or 432) nodes. The system supported LIF and IZH neurons and CUBA exponential, alpha and beta kernels for the synapses and operated with 0.1 ms timestep. The system was targeting general neuromorphic-related applications, such as neuroevolution in the form of AI learning the rules of video games or simulating the cortical microcircuit. The system could simulate up to 110592 neurons. **Hu et al. (2022) [162]** presented an NMA that comprised a systolic array of 4096 PEs. The main characteristic which makes it different from other implementations was the binary systolic array that realized the weights - 0s and 1s reflected the sign of the weight. The system reached an accuracy of 98.67% after 30 time steps on simplified N-MNIST benchmark (16x16 px images) with an SCNN. The system supported an IF neuron model with long-term depression of the synaptic weights capability. The authors reported power consumption of 29pJ/SO with the system clocked at 100 MHz. **Carpegna et al. (2024) [163]** presented **Spiker+** - complete Python-to-FPGA framework for creating SNNs for image inference and other classification tasks, which was a direct continuation of **Spiker**⁷[164]. The framework supported the BPTT learning method through external learning via the Surrogate Gradient method. Architecture-wise, the system comprised three layers of the hierarchical units - network, layer and neuron and supported six different versions of the LIF model (IF to full LIF). The authors chose 6b and 4b fixed-point weights for MNIST benchmark, but the architecture allowed for using different values. The authors tested the architecture with MNIST and SHD benchmarks. For MNIST, the system achieved the accuracy of 96.83% on Xilinx Artix-7 clocked at 100 MHz, with the processing speed of 1282 frames per second.

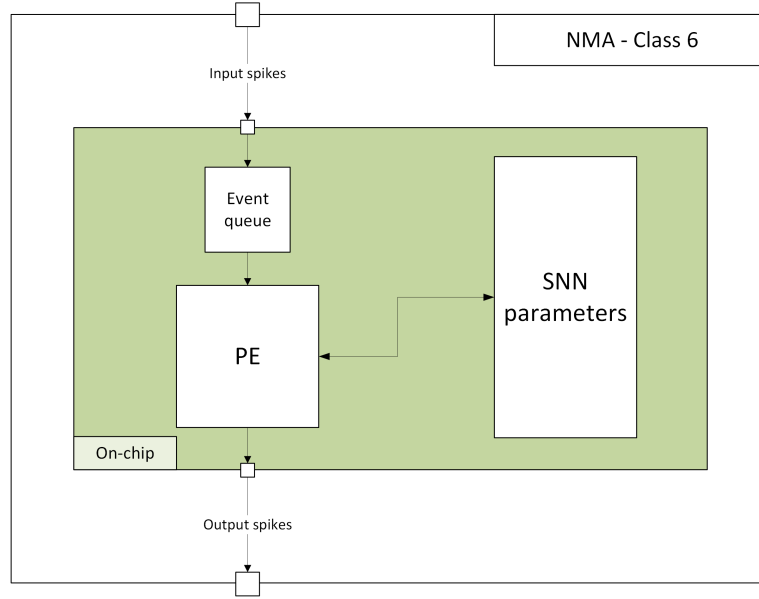


Figure 9. Simplified diagram of a Class 6 NMA.

3.6 Class 5 (Traits: fully parallel, asynchronous network update)

Class 5 architectures support two Traits: fully parallel operation and asynchronous network update. Because the necessary data is stored off-chip, they can support large SNNs and can potentially achieve high operation speeds, due to fully parallel operation and updating the neuron states only if there are spikes. However, those system also bring higher complexity due to need to synchronize asynchronous PEs.

Early modern implementations. **Ipatov et al. (2019) [165]** presented a NoC-based NMA that operated at real-time. Every PE within the NoC allowed for computing up to 512 neurons with a fan-in of 512 synapses. The authors used two Xilinx Kintex-7 devices, which allowed for the implementation of 128 PEs per device. This resulted in the maximum possible number of 131 thousand neurons and 67 million synapses on the platform. All of the above-mentioned data was put on the external DDR3 memory with a capacity of 128 Gb and a total bandwidth of 100 Gbps at 400 MHz.

Modern implementations. **Yang et al. (2021) [166]** presented BiCoSS - a large-scale NMA, designed to simulate parts of the human brain. The system was organized as a multigranular architecture and had a hierarchy of different levels of components. On the top level, the system was organized into nuclei - divided into a set of interconnected SNNs - that exchanged information through a set of external routers. The architecture was arranged in the Butterfly Fat Tree topology (BFT) on the nuclei and neuron levels, but the SNN units were fully interconnected. The SNNs within the nucleus communicated through the roots of the BFTs. The implementation presented in the paper relied on 35 Altera Cyclone-IVs arranged in seven nuclei of five devices (four FPGAs for SNNs, one for routing per nucleus). The architecture supported LIF, IZH and HH neurons and both pair and triplet-wise STDP. The authors tested the system with biology-related tasks, such as decision-making with reinforced learning or context-dependent learning, but also with MNIST benchmark, where it achieved 94.8% accuracy.

3.7 Class 6 (Traits: collocated computation and memory, asynchronous network update)

Class 6 architectures support two Traits: collocated computation and memory and asynchronous network update. They are the closest to fully-neuromorphic systems (Class 7) with the only difference being the lack of fully parallel operation. As the entire system is contained on-chip, they offer high processing speed, but not as fast Class 7, as the number of PEs is lower. Additionally, they should provide lower power consumption due to asynchronous network update. Moreover, they depend to a smaller extent on logic resources than Class 7.

⁷Spiker+ was a newer version of Spiker and, for completeness, we inform that according to the proposed Taxonomy, Spiker is considered Class 1 NMA and is of a much smaller scale.

Early implementations. **Pearson et al. (2005) [167]** presented an architecture composed of multiple TDM PEs. Every PE included a LIF pipeline, handling 120 neurons and 912 synapses. The authors chose a 16b fixed-point number representation and tested the system with a simulation of the basal ganglia. **Cheung et al. (2006) [168]** implemented a Cellular Neural Network realizing a Gabour-type filter for feature extraction from images. The architecture consisted of a 2D array of PEs controlled by a central unit and supported LIF neuron model with the forward Euler integration. The PEs utilized the 16b fixed-point arithmetic. The authors interfaced the system implemented on Xilinx Virtex-II device and clocked at 120 MHz with a 32x32 pixel silicon retina, and the results were presented on the VGA screen. **Cheung et al. (2009) [169]** presented a systolic architecture for the high speed simulation of SNNs, supporting IZH neurons with low neuronal activity. The authors chose a fixed-point 18b number representation for membranes and 9b fixed-point for the weights. The system modeled the random current present in the IZH model equation (as shown in Table 1) with a pseudorandom number generator (based on linear-feedback shift register). The authors tested the system on the Xilinx Virtex-5 device, which they reported could allow for 32 PEs and 848 neurons to be fitted, achieving the performance of 0.73 ms needed for one second of real-time simulation.

Early modern implementations. **Ang et al. (2011) [170]** the authors presented an architecture for an SNN-based auto-associative memory. Topology-wise, it was a single-layer network with interconnects serving as axonal delay elements, which was trained to recall several patterns based on incomplete stimuli. Every neuron was connected to one Coincidence Detector, which in turn were associated with a certain stored pattern and contributed to recurrent activation of this pattern. This design was not based on sequential but rather on combinational logic with customizable delay lines. **Luo et al. (2014) [171]** presented an NMA for simulating human cerebellum network. The system was arranged as a NoC with the maximum support for 100000 neurons on 48 PEs. Every PE comprised two pipelines that would process the data for 20 Golgi cells and 2000 granular cells⁸. The inhibitory connections from Golgi cells to the granule cluster was described with a probability, and, on average, every granule neuron received about eight inhibitory connections, which follows biological observations. Neurons were COBA LIF, with excitatory and inhibitory ion channels. The provided performance figure suggested that the network of 100000 neurons could be processed every 25.6 ms on Xilinx Virtex-7, however the design was only tested with a network of 8000 granular cells and eight Golgi cells on four PEs. **Vangel et al. (2014) [172]** presented an architecture using the Dynamic Neural Field (DNF) to model the neuron-to-neuron interactions. DNF theory describes network activity not based on the dynamics of singular neurons but rather based on approximations of dynamics of large, homogeneous and recurrently connected neural networks based on a mean field approach [173]. From the architectural point of view, the system comprised a 2D grid of PEs interconnected via routers in a NoC-like fashion with a support for stochastic transmission, i.e., the PEs sent out the generated spikes with a given probability. The proposed Randomly Spiking DNF provided local connectivity and distributed, small computation units with four-directional connectivity. The authors implemented the design on a Xilinx Virtex-6 with varying sizes of RSDNF, up to 1200 neurons. **Holanda et al. (2016) [174]** presented DHyANA - a hierarchical NoC-based NMA designed for brain activity simulations. The architecture was a mesh-bus hybrid, with a standard mesh of PEs consisting of clusters of smaller computing elements connected to a shared bus. The clustered smaller computing elements responded to the decoded spike packets read from the common bus. The implementation comprised a 4x4 grid of PEs supporting 208 neurons to be simulated on Altera Stratix-IV, clocked at 56 MHz. **Luo et al. (2016) [175]** presented an architecture with a focus on the collective activity of large groups of neurons, allowing for simulation of up to approx. one million neurons in different configurations. The authors based their approach on the Neural Engineering Framework, which allowed users to construct neural models on a high level of abstraction by defining vectors and functions operating on those vectors. Vectors were groups of neurons, and connections between those groups realized a mathematical function - from simple identity to ODEs. **Lin et al. (2017) [176]** presented an NMA organized as a NoC in tree topology with three supported neuron models - HH, IZH and IF. The NoC structure allowed authors for distributed, partial reconfiguration, which could be used at runtime. Multi-device operation was possible due to the ring topology of interconnected FPGAs. The system was clock-driven, with TDM PEs grouped in clusters with shared memory. **Yang et al. (2019) [177]** presented LaCSNN - a 3D NoC-based NMA utilizing COBA neuron models, which targeted the simulation of a cortico-basal ganglia-thalamocortical network. From an architectural point of view, the system was a NoC

⁸The kind of cells found in cerebellum.

with 36 TDM PEs that supported 4800 virtual neuron updates per timestep in real time. The architecture was by design targeting multi-device systems - in the paper it was a system of six Altera Stratix-III devices, supporting up to around one million neurons and around 60 million synapses in real-time (with average spiking rate of 50 Hz). **Zheng et al. (2019) [178]** presented an NMA arranged as a NoC of 16 PEs. Those PEs were arranged in groups, responsible for specific layers of neurons. The authors tested the system with the MNIST benchmark, with SNN's topology of FF-FC (906 neurons), for which it achieved 98% accuracy. The authors chose an 8b fixed-point number representation for the weights, while the membranes were 13b fixed-point numbers. The LIF neuron implementation relied on a *click-based link-joint circuit* - a 4-signal handshake protocol allowing for asynchronous communication. **Fang et al. (2019) [179, 180]** the authors presented an NMA, arranged as a NoC of TDM PEs supporting LIF neurons and SRM-based synapses. The authors implemented the system on Altera Cyclone-V, which was clocked at 75 MHz. The synaptic potential decay was implemented with a LUT, and the delay of the alpha/dual-exp synapse functions with a shift register. The authors chose a 16b fixed-point number representation for the weights. The authors tested the system with the MNIST benchmark for The FF-FC network of 610 neurons, for which it achieved a 97.7% accuracy. **Mitchell et al. (2020) [181]** presented *μ Caspian* - NMA for SNN simulation targeting low-end FPGAs. The architecture was fully pipelined and allowed for simulating up to 256 LIF neurons and 4096 synapses on Lattice Semiconductor iCE40. The chose the 8b fixed-point number representation for weights. The system supported axonal delay values from zero to 15 timesteps and it was tested with varying sizes of A2A networks (ranging from 10 to about 60 neurons).

Modern implementations. **Nambiar et al. (2020) [182]** presented an NMA arranged as a NoC for neural processing. The NoC comprised of multiple square arrays of PEs of variable size, but the authors presented their results for systems with 64x64, 128x128 and 256x256 arrays (also called *cores*). The system supported only the LIF neuron model, with three available membrane leakage models. The authors chose an 8b fixed-point number representation. They tested the system with MNIST (94% accuracy) and Fisher Iris benchmarks (92.15%). **Sakellariou et al. (2021) [183]** presented a NoC-based NMA supporting LIF neurons with online learning capability performed on a separate ARM core. The learning relied on the continuous approximation of the LIF's transfer function through BP. The system supported XY messaging for communication between PEs. We deduced that the system used a 4x4 array of PEs with 256 neurons that can be simulated on every PE on Xilinx Zynq UltraScale. The system supported axonal delay and featured a 12b weight fixed-point number representation. The system was tested with the MNIST benchmark and FF-FC topology (310 neurons) and achieved 92.15% accuracy. **Nguyen et al. (2021) [184]** presented an architecture for realizing SNNs, with the connection pruning capability. The system supported the IF neurons with time-to-first-spike encoding. The online learning used STDP with an addition of the pruning mechanic, which allowed the system to cut the connections with weights below a predefined threshold. The authors tested the system with an SCNN with three convolution-pooling layers for the Caltech 101 benchmark (95.7% accuracy). **Mack et al. (2021) [185]** presented **RANC** - a complex ecosystem for realizing different NMAs, utilizing a SW/HW co-design approach⁹. In the paper, the authors used it to implement an FPGA-based implementation of IBM TrueNorth[15] - NoC of PEs with crossbars for connectivity, supporting LIF neurons without the refractory period and programmable synaptic delays. The entire paper aimed to prove that the RANC-based TrueNorth[15] was close to the original project, with good performance in CIFAR-10 benchmark, as well as synthetic aperture radar and vector-matrix multiplication applications. **Wang et al. (2022) [187]** presented **TripleBrain** - an NMA consisting of Neural Processing Tiles (NPTs) sharing a common bus, supporting 64 neurons and 1024 synapses per NPT, targeting classification tasks. In the presented implementation, there are four NPTs, resulting in an array of 256 neurons. The architecture realized the concepts of self-organizing maps, STDP and reinforced STDP (R-STDP). The architecture supported single-layer networks, fully connected to the input vector. The system was tested with multiple benchmarks, and it achieved 95.10% accuracy in MNIST with 256 neurons. **Zhao et al. (2023) [188]** presented a system for processing biological signals (neural spikes, EMG, ECG and EEG), which supported them by utilizing different types of neural networks (including SNNs). Architecture-wise, the system comprised four reconfigurable cores connected to a common bus. Each core comprised 16 interconnected PEs with multiple general-purpose datapaths for those different network types. For SNN mode, four PEs realize a single LIF neuron at any given time, resulting in 16 neurons (with 512 synapses) processed simultaneously.

⁹Another RANC-based architecture can be found in [186].

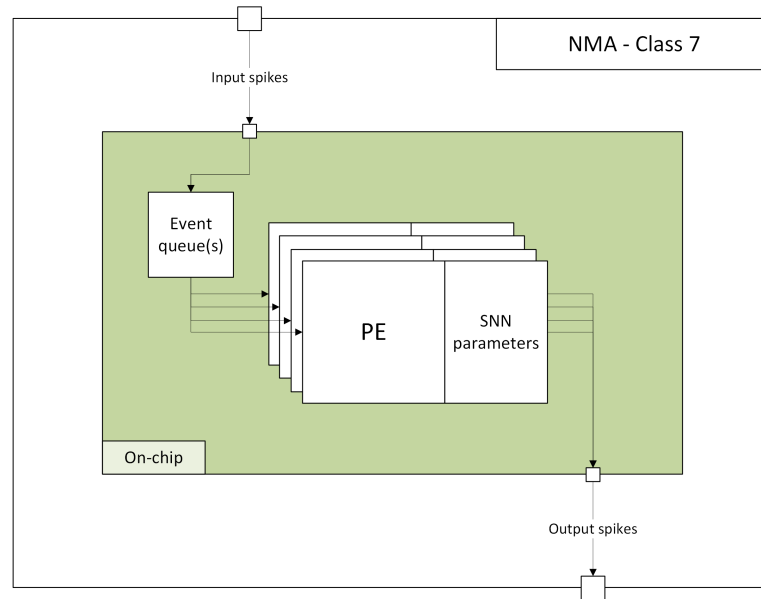


Figure 10. Simplified diagram of a Class 7 NMA.

3.8 Class 7 (Traits: fully parallel, collocated computation and memory, asynchronous network update)

Class 7 architectures support all three Traits, and their operation can be deemed the most *brain-like*. They are also the most bound by the on-chip resources out of all of the Classes, but can allow for the fastest and most energy-efficient operation. However, realizing networks with more than thousands of neurons within this Class is troublesome, due to contemporary FPGAs not being large enough to support such complex and large systems.

Early implementations. **Allen et al. (2005) [189]** presented a platform for pattern recognition in olfactory applications. The system supported IF neuron model with weights uniformly set to 1, so the output spike train of the neuron had a firing rate equal to the average rate of the input spike trains. We deduced that architecture-wise the system was an array of PEs - one for every neuron. The authors reported eight neurons with 1024 input synapses implemented on the Xilinx Virtex-II Pro device. **Girau et al. (2006) [190]** presented an architecture for a Local Excitatory Global Inhibitory Oscillator Network (LEGION)[191], based on IF neurons, for image inference. Architecture-wise, due to the inherent nature of the LEGION-type SNNs, the implementation comprised a 2D array of PEs. Neurons were interconnected with excitatory connections, and there was a single global inhibitor connected to all neurons. The size of the array was equal in size to the size of the image under classification. **Cassidy et al. (2007) [192]** presented a 2D array of LIF neurons capable of realizing Spatio-Temporal Receptive Fields (STRFs), neural parameter optimization algorithms and STDP. The architecture comprised 32 PEs set up as an array, connected to the weight and delay memory. The datapath was time-multiplexed to allow for parallel processing and serial communication. Every neuron was connected to its four neighbors. The system was implemented on Xilinx Spartan-3 device and was clocked at 50 MHz.

Early modern implementations. **Bonabi et al. (2021) [193]** the authors presented a network of 16 HH neurons on a Xilinx Virtex-7 device. The neuronal dynamics were approximated with the CORDIC algorithm and step-by-step time integration. The authors focused on neuronal pools, i.e., groups of interconnected neurons (in A2A fashion) with specific functions, which could be either diffusive or localized. **Dean et al. (2014) [194]** presented **DANNA** - an NMA that comprised an array of multi-purpose *elements* that could be configured to perform a function of a neuron, synapse or fan-in/fan-out connection. The architecture was a 2D grid of *elements*, which be neurons, synapses or fan-out elements. The architecture supported the LIF neuron model with axonal delays. The synapse model supported long-term potentiation and depression for the weights. The network topology was obtained by performing

the genetic algorithm for finding the optimal implementation. The authors tested the system¹⁰ with a randomly connected network of 10000 neurons, implemented on a Xilinx Virtex-7 device with a 9b fixed-point number representation, clocked at eight megahertz, while the *elements* was clocked at 64 MHz. The system was also updated in 2018 and presented as DANNA 2[196]. **Nanami et al. (2016) [197]** presented a modification of an existing Digital Spiking Silicon Neuron (DSSN)[198] idea. The proposed architecture used 16 DSSNs connected to 16 synapse units, each supporting 256 external synapses - all operating at 10x real-time speed. The number representation was 18b. There were no implementation details provided in the paper, so it is difficult to draw any realistic conclusions about the feasibility of this design. **Wilson et al. (2017) [199]** presented **Programmable VHDL Neuron Array (PVNA)** - an NMA with neurons following the modified version of Message-Based Event Driven (MBED)-based neuron model[56]. The architecture relied on a common bus connecting PEs for neurons and synapses with time-multiplexed access. The system supported pausing the simulation for adjusting the system on-the-fly and performing external online learning with STDP. The synapse PEs were daisy-chained with modifiable connections. The implemented system supported a maximum of 100 neurons, 16 pattern generators and 200 synapses on a Xilinx Virtex-5 device and it was tested with a C. Elegans locomotor system simulation with 86 neurons, 6 pattern generators and 180 synapses. **Farsa et al. (2019) [200]** provided a simplified SNN implementation with a focus on minimizing utilization figures. The authors designed it for image inference performed on 5x5 arrays of binary pixels. The neuron model was LIF with simplified operation (1.25 ms timestep and fully multiplierless). The topology was an FF-FC network (6 neurons). The implementation of a single neuron with this architecture could be clocked at 412.371 MHz.

Modern implementations. **Gupta et al. (2020) [201]** presented an architecture for realizing a WTA network for classification tasks. The system comprised 16 PEs, one for every neuron in the output layer of the WTA network, as well as 784 input units for the input spikes related to the pixels. It supported online learning in the form of STDP and fixed-point numerical representation of 24b width. The authors tested the system on Xilinx Virtex-6, where it was clocked at 100 MHz and achieved the inference speed of 2000 frames per second for the MNIST benchmark. **Prashanth et al. (2021) [202]** presented a general view of the implemented architecture, which we deduced to be an accelerator for a particular SCNN with LIF neurons. The architecture used an ARM core for system control and an array of PEs. The paper did not provide any concrete numbers, but we deduced that four PEs were implemented in hardware. The authors also claimed that the system supported STDP. **Wang et al. (2023) [203]** presented an architecture with a specific memory optimization technique, targeting the FF SNNs implementations. They used *ping-pong buffers* to speed up operations. The authors focused on optimizing the sparse spike characteristics: the neuron fan-in was cut into smaller chunks of 64, which were OR'ed to see if there were any spikes incoming. The architecture supported LIF neurons and 256 PEs with one-hot encoding, which the authors claimed increased performance for high levels of connection sparsity (8.84x better performance with 90% sparsity).

3.9 Non-NMA structures related to SNN research

In this section, we present systems that could not be classified as NMAs, presented interesting optimizations of NMAs sub-units or were single neuron implementations. Interested readers are referred to the referenced works.

There is a number of structures that we were not able to fairly compare with the implementations listed in Sections from 3.1 to 3.8, due to the lack of distinctive features of NMAs, as we defined them in Section 2.3. There are many such implementations reported in the literature, and we are listing two of them as examples. **Palumbo et al. (2017) [204]** presented an architecture for simulating Swarm Intelligence (SI) using SNNs, it employed a soft-core processor and a designated coprocessor to provide a systolic array for realizing partial calculations for neuronal dynamics. **Shahsavari et al. (2021)** presented **Partially Ordered Event-Triggered System (POETS)** architecture - a general-purpose parallel architecture of a number of RISC-V cores arranged in a NoC on multiple FPGAs.

In many papers, the authors were focusing on optimizing parts of NMAs. As an interested reader may find information on optimizing specific their NMA designs extremely useful, we list such papers, grouped by the sub-units being optimized: spike encoding - [205], exponential function unit - [206], STDP-based learning - [207, 208, 209, 210], ion channel dynamics unit - [211, 212], soma unit - [213], alternative to

¹⁰There were many examples of the use cases for this architecture, including NeoN[195], which was a neuromorphic control for autonomous robotic navigation.

SNN-based processing (P systems) - [214].

While surveying the neuromorphic architectures, we realized that many researchers were focusing on implementing single neurons on FPGAs with hardware optimizations, accuracy of simulation and biological plausibility of the results in mind. Examples of such works, grouped by the neuron model the authors aimed at implementing, are as follows: HH - [215, 216], LIF - [217], AdEx - [218, 219], HR - [220, 221, 222], ML - [223], IZH - [224, 225], WIL - [226], Pinsky-Rinzel (PR) - [227], multiple - [228], other - [229].

4 TRENDS, TENDENCIES, AND DISCUSSION

We surveyed 129 papers describing NMAs that provided enough information for us to apply the Taxonomy rules and derive further metrics. Additional 27 papers consisted of non-NMA structures and NMA-related research, as described in Section 3.9. Around 86.78% of architecture featured a parallel architecture, with 30.58% being fully parallel. Some form of online learning was featured in 31.4% of implementations, which is a rather small number - most likely due to the lack of agreement on how to realize brain-like learning in hardware efficiently. As Figure 11 suggests, the NMAs on FPGAs have been gaining popularity throughout the years, with the most implementations presented around the year 2021. We can see that the three most populous classes are Class 2 (38), Class 4 (22) and Class 6 (17). This is unsurprising as the collocated memory and computation is the easiest Trait to include, and thus we can see them appearing often. Class 7 consists of only 10 examples, but they can also be seen throughout the years, showing interest in implementing *fully neuromorphic* systems. Close to 53.5% of the NMAs realized up to and including 1000 neurons. This can be due to the classification tasks being the most popular use case – 40% of NMAs according to the Figure 14 – and those do not require large networks. The target benchmarks should be thus reconsidered and new ones should be introduced to test more complex NMAs. Moreover, 28% of architectures target neuroscience, reinforcing the close connection between biological and spiking neural networks. The most popular neuron model is LIF (47.29%), followed by IZH (18.6%), IF (14.7%) and HH (9.3%) - the rest of the models were utilized in around 10% of the architectures. As LIF neurons are the simplest to implement, IZH give similar spiking behaviors with reduced complexity to the complete and HH neurons are popular for neuroscientific experiments - those results are not surprising. The hardware constraints were a crucial factor when selecting the appropriate neuron model and not many researchers decided to implement the complex HH model. The most popular topology is FF-FC (33.3%), then SCNN (12.4%), A2A (10.9%), biology-related "fixed" topologies (8.5%), WTA (7%) and LSMs (2.3%) - other topologies were usually special cases with a single representative. Once again, the influence of the use case in topology choice is rather apparent. Interestingly, a majority of NMAs (86%) were implemented on Xilinx/AMD devices, which may suggest that FPGA-based NMAs development is dependent on a single manufacturer when it comes for creating larger and faster implementations. Moreover, nearly 77% of the architectures utilized at most 50% of the available resources, regardless of the platform size and manufacturer, and there were only five examples of systems clocked at above 200 MHz, which suggests that even today the FPGAs are not utilized to their full potential in the field of NMA development. Figure 15 shows the trend of available logic resources on FPGAs, based on the size of the AMD/Xilinx Virtex FPGA device family¹¹ (black dots) through the years and required logic resources for implementing 10^{11} neurons – the estimated size of the human brain – on a single chip for the most promising architectures from every Class. We can see that, if we discard the impact of embedded memory size and improvements in on-chip communication and assume this trend to hold, Classes 0 and 3 can be expected to achieve human-brain scale around the year 2035 as they require the least amount of on-chip logic resources and scale the best in single-chip implementations. The rest need more time – Classes 1, 2, 4, 6 and 7 would achieve the goal after 2055 and Class 5 (prediction is rather vague here, because it is based on a system that used multiple FPGAs – BiCoSS) would achieve it after 2045. They would benefit more from adding more chips, as it is already being done[230]. However, considering that IEEE suggests in their International Roadmap for Devices and Systems (IRDS) from 2022 that Moore's Law will be upheld for additional 10-15 years[231], only Classes 0 and 3 seem likely to achieve the aforementioned goal in the predicted years.

¹¹The newest devices from AMD - Versal - are discarded as they are not *pure* FPGAs, but rather System-On-a-Chip devices with relatively small FPGA fabric (as a percentage of the entire chip).

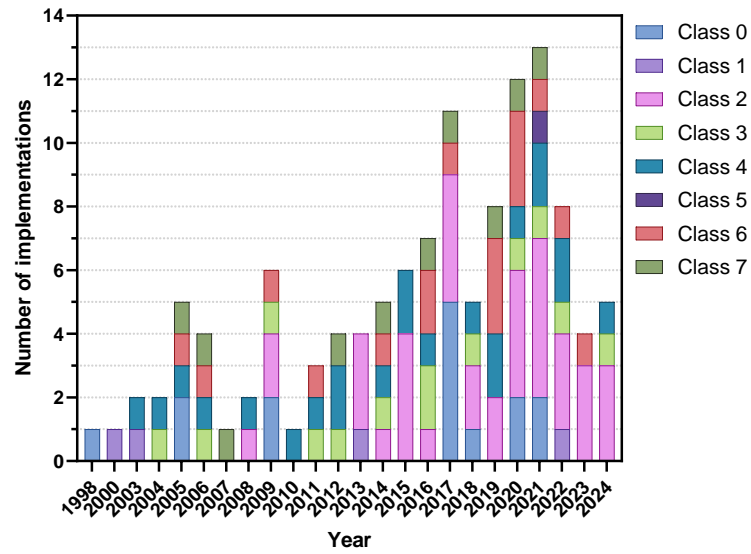


Figure 11. Class population structure through years.

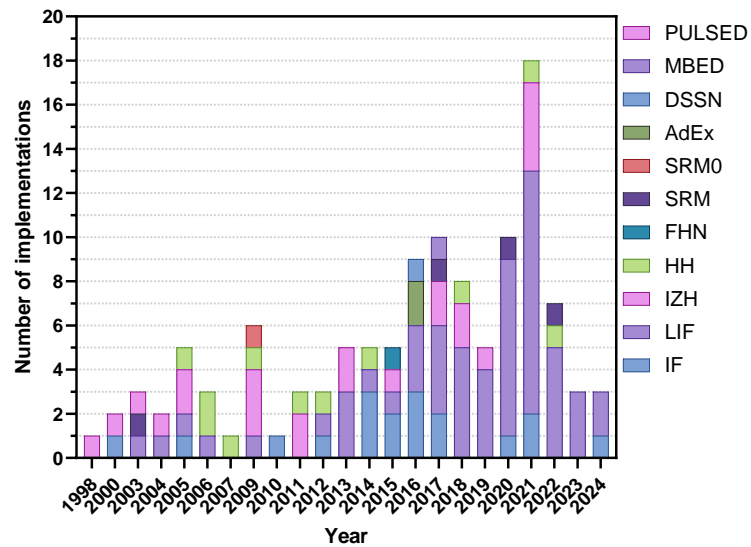


Figure 12. Share of different neuron models through years.

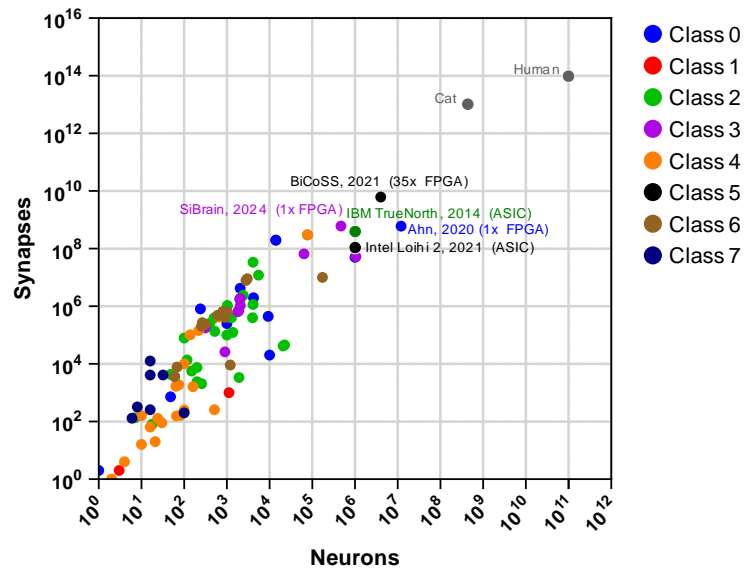


Figure 13. Complexity of the implemented architectures.

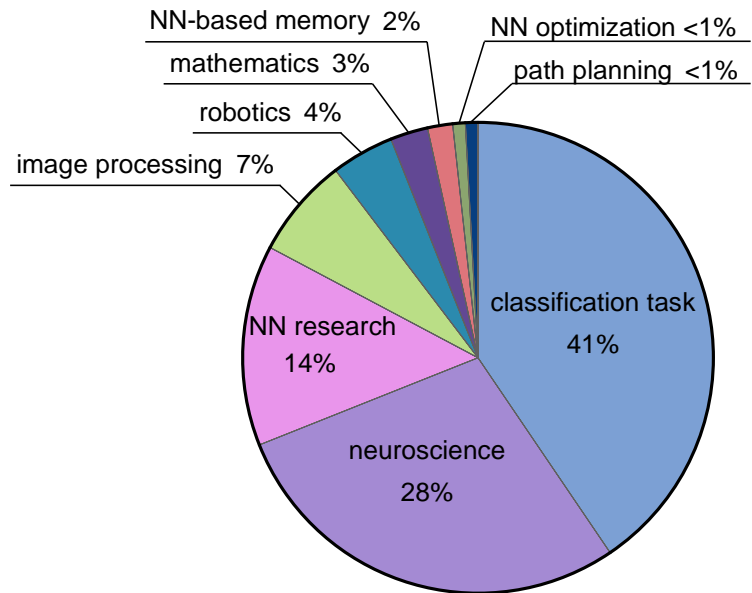


Figure 14. Share of use cases for the surveyed architectures.

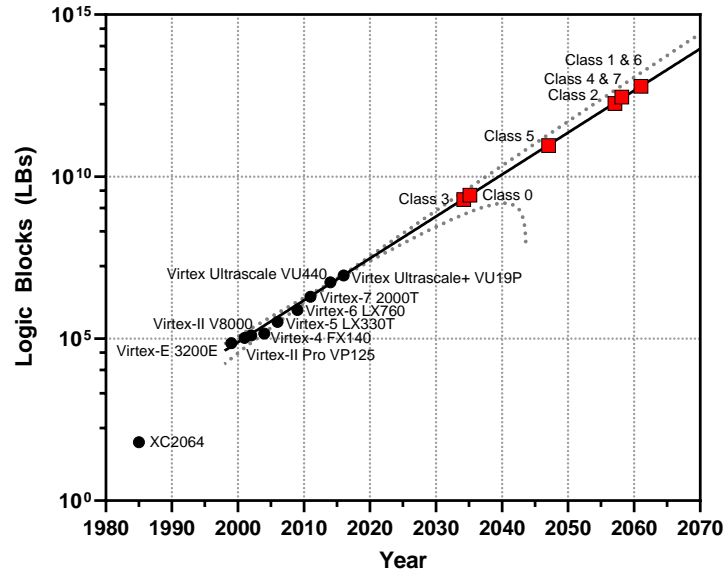


Figure 15. Predicted LB number required to implement 10^{11} of neurons on an FPGA by Class.

5 CONCLUSION

The FPGA-based neuromorphic systems can be implemented in various ways, with different advantages and disadvantages, which is reflected by the Classes of the Taxonomy we provided. Representatives of those Classes fit diverse sets of requirements and allow for achieving diverse goals - from classification tasks to neuroscientific simulations. We expect that the popularity of the digital NMAs will continue to grow and that even more brain-like systems will be presented, as new discoveries related to human brain are made. Moreover, it is apparent, due to the stark differences in design choices between the Classes, that creating a unified Design Space Exploration framework that would allow for convenient and automatic search of optimal architectural Class for given requirements (e.g., number of neurons, synapses, neuron models and available FPGA platform) is troublesome, but we believe it is necessary in order to simplify the NMA design process.

ACKNOWLEDGMENTS

This work was supported by Swedish Research Council's Project Building Digital Brains under Grant 2021-04579.

REFERENCES

- [1] R. R. Schaller, "Moore's law: past, present and future," *IEEE spectrum*, vol. 34, no. 6, pp. 52–59, 1997.
- [2] M. Bohr, "A 30 year retrospective on Dennard's MOSFET scaling paper," *IEEE Solid-State Circuits Society Newsletter*, vol. 12, no. 1, pp. 11–13, 2007.
- [3] R. H. Dennard, J. Cai, and A. Kumar, "A perspective on today's scaling challenges and possible future directions," in *Handbook of thin film deposition*, pp. 3–18, Elsevier, 2018.
- [4] H. Esmailzadeh, E. Blem, R. St. Amant, K. Sankaralingam, and D. Burger, "Dark silicon and the end of multicore scaling," in *Proceedings of the 38th annual international symposium on Computer architecture*, pp. 365–376, 2011.
- [5] J. Shalf, "The future of computing beyond Moore's Law," *Philosophical Transactions of the Royal Society A*, vol. 378, no. 2166, p. 20190061, 2020.
- [6] C. E. Leiserson, N. C. Thompson, J. S. Emer, B. C. Kuszmaul, B. W. Lampson, D. Sanchez, and T. B. Schardl, "There's plenty of room at the Top: What will drive computer performance after Moore's law?," *Science*, vol. 368, no. 6495, p. eaam9744, 2020.

- [7] L. Gyongyosi and S. Imre, "A survey on quantum computing technology," *Computer Science Review*, vol. 31, pp. 51–71, 2019.
- [8] R. Bommi and R. S. Selvakumar, "A survey on adiabatic logic families for implementing reversible logic circuits," in *2018 IEEE international conference on computational intelligence and computing research (ICCIC)*, pp. 1–4, IEEE, 2018.
- [9] B. J. MacLennan, "A review of analog computing," *Department of Electrical Engineering & Computer Science, University of Tennessee, Technical Report UT-CS-07-601 (September)*, pp. 19798–19807, 2007.
- [10] C. D. Schuman, T. E. Potok, R. M. Patton, J. D. Birdwell, M. E. Dean, G. S. Rose, and J. S. Plank, "A survey of neuromorphic computing and neural networks in hardware," *arXiv preprint arXiv:1705.06963*, 2017.
- [11] A. Podobas, K. Sano, and S. Matsuoka, "A survey on coarse-grained reconfigurable architectures from a performance perspective," *IEEE access : practical innovations, open solutions*, vol. 8, pp. 146719–146743, 2020.
- [12] I. Kuon, R. Tessier, J. Rose, and others, "FPGA architecture: Survey and challenges," *Foundations and Trends® in Electronic Design Automation*, vol. 2, no. 2, pp. 135–253, 2008.
- [13] C. Mead, "Neuromorphic electronic systems," *Proceedings of the IEEE*, vol. 78, no. 10, pp. 1629–1636, 1990.
- [14] M. Davies, N. Srinivasa, T.-H. Lin, G. Chinya, Y. Cao, S. H. Choday, G. Dimou, P. Joshi, N. Imam, S. Jain, and others, "Loihi: A neuromorphic manycore processor with on-chip learning," *Ieee Micro*, vol. 38, no. 1, pp. 82–99, 2018.
- [15] F. Akopyan, J. Sawada, A. Cassidy, R. Alvarez-Icaza, J. Arthur, P. Merolla, N. Imam, Y. Nakamura, P. Datta, G.-J. Nam, and others, "Truenorth: Design and tool flow of a 65 mw 1 million neuron programmable neurosynaptic chip," *IEEE transactions on computer-aided design of integrated circuits and systems*, vol. 34, no. 10, pp. 1537–1557, 2015.
- [16] A. Neckar, S. Fok, B. V. Benjamin, T. C. Stewart, N. N. Oza, A. R. Voelker, C. Eliasmith, R. Manohar, and K. Boahen, "Braindrop: A mixed-signal neuromorphic architecture with a dynamical systems-based programming model," *Proceedings of the IEEE*, vol. 107, no. 1, pp. 144–164, 2018.
- [17] G. Indiveri, B. Linares-Barranco, T. J. Hamilton, A. v. Schaik, R. Etienne-Cummings, T. Delbruck, S.-C. Liu, P. Dudek, P. Häfliger, S. Renaud, and others, "Neuromorphic silicon neuron circuits," *Frontiers in neuroscience*, vol. 5, p. 73, 2011.
- [18] Y. Li, Z. Wang, R. Midya, Q. Xia, and J. J. Yang, "Review of memristor devices in neuromorphic computing: materials sciences and device challenges," *Journal of Physics D: Applied Physics*, vol. 51, no. 50, p. 503002, 2018.
- [19] B. J. Shastri, A. N. Tait, T. Ferreira de Lima, W. H. Pernice, H. Bhaskaran, C. D. Wright, and P. R. Prucnal, "Photonics for artificial intelligence and neuromorphic computing," *Nature Photonics*, vol. 15, no. 2, pp. 102–114, 2021.
- [20] W. Maass, "Networks of spiking neurons: the third generation of neural network models," *Neural networks*, vol. 10, no. 9, pp. 1659–1671, 1997.
- [21] M. Davies, A. Wild, G. Orchard, Y. Sandamirskaya, G. A. F. Guerra, P. Joshi, P. Plank, and S. R. Risbud, "Advancing neuromorphic computing with loihi: A survey of results and outlook," *Proceedings of the IEEE*, vol. 109, no. 5, pp. 911–934, 2021.
- [22] R. S. Nikhil, "Can dataflow subsume von Neumann computing?," in *Proceedings of the 16th annual international symposium on Computer architecture*, pp. 262–272, 1989.
- [23] S. Song, K. D. Miller, and L. F. Abbott, "Competitive Hebbian learning through spike-timing-dependent synaptic plasticity," *Nature neuroscience*, vol. 3, no. 9, pp. 919–926, 2000.
- [24] N. Ravichandran, A. Lansner, and P. Herman, "Unsupervised representation learning with Hebbian synaptic and structural plasticity in brain-like feedforward neural networks," *arXiv preprint arXiv:2406.04733*, 2024.
- [25] G. Bellec, F. Scherr, A. Subramoney, E. Hajek, D. Salaj, R. Legenstein, and W. Maass, "A solution to the learning dilemma for recurrent networks of spiking neurons," *Nature communications*, vol. 11, no. 1, p. 3625, 2020.
- [26] S. Gandhare and B. Karthikeyan, "Survey on FPGA architecture and recent applications," in *2019 international conference on vision towards emerging trends in communication and networking*

- (ViTECoN), pp. 1–4, IEEE, 2019.
- [27] Juan Jose Rodriguez Andina, E. D. I. T. Arnanz, and M. D. V. Pe{\~n}a, *FPGAs: fundamentals, advanced features, and applications in industrial electronics*. CRC Press, 2017.
 - [28] A. Jacobs, G. Cieslewski, A. D. George, A. Gordon-Ross, and H. Lam, “Reconfigurable fault tolerance: A comprehensive framework for reliable and adaptive FPGA-based space computing,” *ACM Transactions on Reconfigurable Technology and Systems (TRETS)*, vol. 5, no. 4, pp. 1–30, 2012.
 - [29] J. Weerasinghe, F. Abel, C. Hagleitner, and A. Herkersdorf, “Enabling FPGAs in hyperscale data centers,” in *2015 IEEE 12th intl conf on ubiquitous intelligence and computing and 2015 IEEE 12th intl conf on autonomic and trusted computing and 2015 IEEE 15th intl conf on scalable computing and communications and its associated workshops (UIC-ATC-ScalCom)*, pp. 1078–1086, IEEE, 2015.
 - [30] H. Calderón, C. Elena, and S. Vassiliadis, “Soft core processors and embedded processing: a survey and analysis,” in *Proceedings of-ProRISC*, pp. 483–488, 2005.
 - [31] K. Andryc, M. Merchant, and R. Tessier, “FlexGrip: a soft GPGPU for fpgas,” in *2013 international conference on field-programmable technology (FPT)*, pp. 230–237, IEEE, 2013.
 - [32] A. Podobas and S. Matsuoka, “Designing and accelerating spiking neural networks using OpenCL for FPGAs,” in *2017 international conference on field programmable technology (ICFPT)*, pp. 255–258, IEEE, 2017.
 - [33] X. Ju, B. Fang, R. Yan, X. Xu, and H. Tang, “An FPGA implementation of deep spiking neural networks for low-power and fast classification,” *Neural computation*, vol. 32, no. 1, pp. 182–204, 2020.
 - [34] B. A. Lindqvist and A. Podobas, “Fast algorithms for spiking neural network simulation with fpgas,” *arXiv preprint arXiv:2405.02019*, 2024.
 - [35] A. Shrestha, H. Fang, Z. Mei, D. P. Rider, Q. Wu, and Q. Qiu, “A survey on neuromorphic computing: Models and hardware,” *IEEE Circuits and Systems Magazine*, vol. 22, no. 2, pp. 6–35, 2022.
 - [36] M. Maślanka and M. Gorgoń, “A survey of FPGA implementations of artificial spiking neurons models,” *Bio-Algorithms and Med-Systems*, vol. 8, no. 1, p. 77, 2012.
 - [37] A. Mehrabi and A. van Schaik, “FPGA-based spiking neural networks,” 2024.
 - [38] L. P. Maguire, T. M. McGinnity, B. Glackin, A. Ghani, A. Belatreche, and J. Harkin, “Challenges for large-scale implementations of spiking neural networks on FPGAs,” *Neurocomputing*, vol. 71, no. 1-3, pp. 13–29, 2007.
 - [39] A. Podobas, H. R. Zohouri, N. Maruyama, and S. Matsuoka, “Evaluating high-level design strategies on FPGAs for high-performance computing,” in *2017 27th international conference on field programmable logic and applications (FPL)*, pp. 1–4, IEEE, 2017.
 - [40] H. R. Zohouri, N. Maruyama, A. Smith, M. Matsuda, and S. Matsuoka, “Evaluating and optimizing OpenCL kernels for high performance computing with FPGAs,” in *SC’16: Proceedings of the international conference for high performance computing, networking, storage and analysis*, pp. 409–420, IEEE, 2016.
 - [41] R. Nane, V.-M. Sima, C. Pilato, J. Choi, B. Fort, A. Canis, Y. T. Chen, H. Hsiao, S. Brown, F. Ferrandi, and others, “A survey and evaluation of FPGA high-level synthesis tools,” *IEEE Transactions on Computer-Aided Design of Integrated Circuits and Systems*, vol. 35, no. 10, pp. 1591–1604, 2015.
 - [42] T. C. Potjans and M. Diesmann, “The cell-type specific cortical microcircuit: relating structure and activity in a full-scale spiking network model,” *Cerebral cortex*, vol. 24, no. 3, pp. 785–806, 2014.
 - [43] M. L. Hines and N. T. Carnevale, “The NEURON simulation environment,” *Neural computation*, vol. 9, no. 6, pp. 1179–1209, 1997.
 - [44] M.-O. Gewaltig and M. Diesmann, “Nest (neural simulation tool),” *Scholarpedia*, vol. 2, no. 4, p. 1430, 2007.
 - [45] M. Stimberg, R. Brette, and D. F. Goodman, “Brian 2, an intuitive and efficient neural simulator,” *elife*, vol. 8, p. e47314, 2019.
 - [46] W. Maass, “Liquid state machines: motivation, theory, and applications,” *Computability in context: computation and logic in the real world*, pp. 275–296, 2011. Publisher: World Scientific.
 - [47] D. M. Wilson, “The central nervous control of flight in a locust,” *Journal of Experimental Biology*,

- vol. 38, no. 2, pp. 471–490, 1961. Publisher: The Company of Biologists Ltd.
- [48] E. Jankowska and W. Roberts, “An electrophysiological demonstration of the axonal projections of single spinal interneurons in the cat,” *The Journal of Physiology*, vol. 222, no. 3, pp. 597–622, 1972. Publisher: Wiley Online Library.
 - [49] M. Mahowald, *An analog VLSI system for stereoscopic vision*, vol. 265. Springer Science & Business Media, 1994.
 - [50] E. M. Izhikevich, “Which model to use for cortical spiking neurons?,” *IEEE transactions on neural networks*, vol. 15, no. 5, pp. 1063–1070, 2004.
 - [51] G. P. Sarma, C. W. Lee, T. Portegys, V. Ghayoomie, T. Jacobs, B. Alicea, M. Cantarelli, M. Currie, R. C. Gerkin, S. Gingell, and others, “OpenWorm: overview and recent advances in integrative biological simulation of *Caenorhabditis elegans*,” *Philosophical Transactions of the Royal Society B*, vol. 373, no. 1758, p. 20170382, 2018.
 - [52] P. U. Diehl and M. Cook, “Unsupervised learning of digit recognition using spike-timing-dependent plasticity,” *Frontiers in computational neuroscience*, vol. 9, p. 99, 2015.
 - [53] A. L. Hodgkin and A. F. Huxley, “A quantitative description of membrane current and its application to conduction and excitation in nerve,” *The Journal of physiology*, vol. 117, no. 4, p. 500, 1952.
 - [54] W. Gerstner, W. M. Kistler, R. Naud, and L. Paninski, *Neuronal dynamics: From single neurons to networks and models of cognition*. Cambridge University Press, 2014.
 - [55] J. T. A. Waldemark, T. Lindblad, C. S. Lindsey, K. E. Waldemark, J. Öberg, and M. Millberg, “Pulse coupled neural network implementation in FPGA,” vol. 3390, pp. 392–402, SPIE, 1998.
 - [56] E. T. Claverol, *An event-driven approach to biologically realistic simulation of neural aggregates*. PhD Thesis, University of Southampton, 2000.
 - [57] R. D. Traub, R. K. Wong, R. Miles, and H. Michelson, “A model of a CA3 hippocampal pyramidal neuron incorporating voltage-clamp data on intrinsic conductances,” *Journal of neurophysiology*, vol. 66, no. 2, pp. 635–650, 1991.
 - [58] F. A. Azevedo, L. R. Carvalho, L. T. Grinberg, J. M. Farfel, R. E. Ferretti, R. E. Leite, W. J. Filho, R. Lent, and S. Herculano-Houzel, “Equal numbers of neuronal and nonneuronal cells make the human brain an isometrically scaled-up primate brain,” *Journal of Comparative Neurology*, vol. 513, no. 5, pp. 532–541, 2009. Publisher: Wiley Online Library.
 - [59] Y. Ben-Ari, R. Khazipov, X. Leinekugel, O. Caillard, and J.-L. Gaiarsa, “GABAA, NMDA and AMPA receptors: a developmentally regulated ménage à trois,” *Trends in neurosciences*, vol. 20, no. 11, pp. 523–529, 1997.
 - [60] A. Citri and R. C. Malenka, “Synaptic plasticity: multiple forms, functions, and mechanisms,” *Neuropsychopharmacology : official publication of the American College of Neuropsychopharmacology*, vol. 33, no. 1, pp. 18–41, 2008.
 - [61] W. Gerstner, “Hebbian learning and plasticity,” *From neuron to cognition via computational neuroscience*, pp. 0–25, 2011.
 - [62] E. L. Bienenstock, L. N. Cooper, and P. W. Munro, “Theory for the development of neuron selectivity: orientation specificity and binocular interaction in visual cortex,” *Journal of Neuroscience*, vol. 2, no. 1, pp. 32–48, 1982.
 - [63] S. M. Bohte, J. N. Kok, and J. A. La Poutré, “SpikeProp: backpropagation for networks of spiking neurons,” in *ESANN*, vol. 48, pp. 419–424, Bruges, 2000.
 - [64] P. J. Werbos, “Generalization of backpropagation with application to a recurrent gas market model,” *Neural Networks*, vol. 1, no. 4, pp. 339–356, 1988.
 - [65] J. Kaiser, H. Mostafa, and E. Neftci, “Synaptic plasticity dynamics for deep continuous local learning (DECOLLE),” *Frontiers in Neuroscience*, vol. 14, p. 424, 2020.
 - [66] C. D. Schuman, S. R. Kulkarni, M. Parsa, J. P. Mitchell, P. Date, and B. Kay, “Opportunities for neuromorphic computing algorithms and applications,” *Nature Computational Science*, vol. 2, no. 1, pp. 10–19, 2022.
 - [67] D. B. Skillicorn, “A taxonomy for computer architectures,” *Computer*, vol. 21, no. 11, pp. 46–57, 1988.
 - [68] D. Jung, N. Mehrtash, and H. Klar, “Advanced dedicated hardware for simulating biologically inspired neural networks,” vol. 2005, pp. 1737–1740, 2005.
 - [69] N. Mehrtash, D. Jung, H. H. Hellmich, T. Schoenauer, V. T. Lu, and H. Klar, “Synaptic plasticity in spiking neural networks (SP/sup 2/INN): a system approach,” *IEEE transactions on neural*

- networks, vol. 14, no. 5, pp. 980–992, 2003.
- [70] B. Glackin, T. M. McGinnity, L. P. Maguire, Q. Wu, and A. Belatreche, “A novel approach for the implementation of large scale spiking neural networks on FPGA hardware,” in *Computational Intelligence and Bioinspired Systems, Proceedings* (J. Cabestany, A. Prieto, and F. Sandoval, eds.), vol. 3512 of *Lecture Notes in Computer Science*, pp. 552–563, 2005.
 - [71] B. Glackin, L. P. Maguire, T. M. McGinnity, A. Belatreche, and Q. Wu, *Implementation of a biologically realistic spiking neuron model on FPGA hardware*. Proceedings of the 8th Joint Conference on Information Sciences, Vols 1-3, 2005.
 - [72] M. A. Nuno-Maganda, M. Arias-Estrada, C. Torres-Huitzil, and B. Girau, “Hardware implementation of Spiking Neural Network classifiers based on backpropagation-based learning algorithms,” pp. 2294–2301, 2009.
 - [73] K. L. Rice, M. A. Bhuiyan, T. M. Taha, C. N. Vutsinas, M. C. Smith, and Ieee, *FPGA Implementation of Izhikevich Spiking Neural Networks for Character Recognition*. 2009 International Conference on Reconfigurable Computing and Fpgas, 2009.
 - [74] H. Mostafa, B. U. Pedroni, S. Sheik, and G. Cauwenberghs, “Fast classification using sparsely active spiking networks,” Institute of Electrical and Electronics Engineers Inc., 2017.
 - [75] F. Galindo Sanchez and J. Nunez-Yanez, “Energy proportional streaming spiking neural network in a reconfigurable system,” *Microprocessors and Microsystems*, vol. 53, pp. 57–67, 2017.
 - [76] E. Kousanakis, A. Dollas, E. Sotiriades, I. Papaefstathiou, D. N. Pnevmatikatos, A. Papoutsis, P. C. Petrantonakis, P. Poirazi, S. Chavlis, G. Kastellakis, and Ieee, *An Architecture for the Acceleration of a Hybrid Leaky Integrate and Fire SNN on the Convey HC-2ex FPGA-Based Processor*. 2017 Ieee 25th Annual International Symposium on Field-Programmable Custom Computing Machines, 2017.
 - [77] A. J. Humaidi and T. M. Kadhim, “Spiking versus traditional neural networks for character recognition on FPGA platform,” *Journal of Telecommunication, Electronic and Computer Engineering*, vol. 10, no. 3, pp. 109–115, 2018.
 - [78] B. Ahn, “Implementation of a 12-Million Hodgkin-Huxley Neuron Network on a Single Chip,” Association for Computing Machinery, 2020.
 - [79] M. Ogaki and Y. Sato, “Hodgkin-Huxley-Based Neural Simulation with Networks Connecting to Near-Neighbor Neurons,” in *2021 IEEE 32nd International Conference on Application-specific Systems, Architectures and Processors (ASAP)*, pp. 109–116, July 2021.
 - [80] K. Cheung, S. R. Schultz, and W. Luk, “NeuroFlow: A general purpose spiking neural network simulation platform using customizable processors,” *Frontiers in Neuroscience*, vol. 9, no. JAN, 2016.
 - [81] K. Cheung, S. R. Schultz, and W. Luk, “A large-scale spiking neural network accelerator for FPGA systems,” vol. 7552 LNCS, pp. 113–120, 2012.
 - [82] P. Zhou and S. Hu, “A Neuromorphic Computing Platform with Compact Neuromorphic Core,” in *2021 IEEE 3rd International Conference on Circuits and Systems (ICCS)*, pp. 273–276, Oct. 2021.
 - [83] S. Maya, R. Reynoso, C. Torres, and M. Arias-Estrada, “Compact spiking neural network implementation in FPGA,” *Lecture Notes in Computer Science (including subseries Lecture Notes in Artificial Intelligence and Lecture Notes in Bioinformatics)*, vol. 1896, pp. 270–276, 2000.
 - [84] J. M. Xicotencatl and M. Arias-Estrada, “FPGA based high density spiking neural network array,” in *Lecture Notes in Computer Science (including subseries Lecture Notes in Artificial Intelligence and Lecture Notes in Bioinformatics)* (P. Y. K. Cheung, G. A. Constantinides, and J. T. de Sousa, eds.), vol. 2778, pp. 1053–1056, Springer Verlag, 2003.
 - [85] J. C. Moctezuma, J. P. McGeehan, and J. L. Nunez-Yanez, “Numerically efficient and biophysically accurate neuroprocessing platform,” in *2013 International Conference on Reconfigurable Computing and FPGAs (ReConFig)*, pp. 1–6, 2013.
 - [86] B. Schrauwen, M. D’Haene, D. Verstraeten, and J. V. Campenhout, “Compact hardware liquid state machines on FPGA for real-time speech recognition,” *Neural Networks*, vol. 21, no. 2-3, pp. 511–523, 2008.
 - [87] D. Thomas and W. Luk, “FPGA Accelerated Simulation of Biologically Plausible Spiking Neural Networks,” in *2009 17th IEEE Symposium on Field Programmable Custom Computing Machines*, pp. 45–52, 2009.
 - [88] M. Wildie, W. Luk, S. R. Schultz, P. H. W. Leong, and A. K. Fidjeland, “Reconfigurable acceleration

- of neural models with gap junctions,” pp. 439–442, 2009.
- [89] M. Ambroise, T. Levi, Y. Bornat, and S. Saighi, “Biorealistic spiking neural network on FPGA,” in *2013 47th Annual Conference on Information Sciences and Systems (CISS)*, pp. 1–6, 2013.
 - [90] M. Ambroise, T. Levi, S. Joucla, B. Yvert, and S. Saighi, “Real-time biomimetic central pattern generators in an FPGA for hybrid experiments,” *Frontiers in Neuroscience*, no. 7 NOV, 2013.
 - [91] R. Wang, G. Cohen, K. M. Stiefel, T. J. Hamilton, J. Tapson, and A. Van Schaik, “An FPGA implementation of a polychronous spiking neural network with delay adaptation,” *Frontiers in Neuroscience*, no. 7 FEB, 2013.
 - [92] S. Yang, J. Wang, S. Li, B. Deng, X. Wei, H. Yu, and H. Li, “Cost-efficient FPGA implementation of basal ganglia and their Parkinsonian analysis,” *Neural Netw.*, vol. 71, no. C, pp. 62–75, 2015.
 - [93] J. Wang, S. Yang, B. Deng, X. Wei, and H. Yu, “Multi-FPGA implementation of feedforward network and its performance analysis,” vol. 2015-September, pp. 3457–3461, IEEE Computer Society, 2015.
 - [94] B. Ahn, “Neuron-like digital hardware architecture for large-scale neuromorphic computing,” vol. 2015-September, Institute of Electrical and Electronics Engineers Inc., 2015.
 - [95] J. L. Molin, T. Figliolia, K. Sanni, I. Doxas, A. Andreou, and R. Etienne-Cummings, “FPGA emulation of a spike-based, stochastic system for real-time image dewarping,” vol. 2015-September, Institute of Electrical and Electronics Engineers Inc., 2015.
 - [96] F. Shafait and T. M. Breuel, “Document image dewarping contest,” in *2nd Int. Workshop on Camera-Based Document Analysis and Recognition, Curitiba, Brazil*, pp. 181–188, Citeseer, 2007.
 - [97] W. Lei, L. Yuling, S. Shuxiang, J. Harkin, and L. Junxiu, “Efficient neuron architecture for FPGA-based spiking neural networks,” in *2016 27th Irish Signals and Systems Conference (ISSC)*, pp. 1–6, 2016.
 - [98] B. Shao and P. Li, “Array-based approximate arithmetic computing: A general model and applications to multiplier and squarer design,” *IEEE Transactions on Circuits and Systems I: Regular Papers*, vol. 62, no. 4, pp. 1081–1090, 2015.
 - [99] B. Shao and P. Li, “A model for array-based approximate arithmetic computing with application to multiplier and squarer design,” in *Proceedings of the 2014 international symposium on Low power electronics and design*, pp. 9–14, 2014.
 - [100] D. Pani, P. Meloni, G. Tuveri, F. Palumbo, P. Massobrio, and L. Raffo, “An FPGA platform for real-time simulation of spiking neuronal networks,” *Frontiers in Neuroscience*, vol. 11, 2017.
 - [101] Q. Y. Sun, Q. X. Wu, X. Wang, and L. Hou, “A spiking neural network for extraction of features in colour opponent visual pathways and FPGA implementation,” *Neurocomputing*, vol. 228, pp. 119–132, 2017.
 - [102] C. S. Thakur, J. Molin, and R. Etienne-Cummings, “Real-time image segmentation using a spiking neuromorphic processor,” Institute of Electrical and Electronics Engineers Inc., 2017.
 - [103] J. L. Molin, A. Eisape, C. S. Thakur, V. Varghese, C. Brandli, and R. Etienne-Cummings, “Low-power, low-mismatch, highly-dense array of VLSI Mihalas-Niebur neurons,” in *2017 IEEE International Symposium on Circuits and Systems (ISCAS)*, pp. 1–4, IEEE, 2017.
 - [104] M. Jalilian, M. Nouri, A. Ahmadi, and N. Kandalafi, “Pulse width modulation (PWM) signals using spiking neuronal networks,” pp. 180–184, Institute of Electrical and Electronics Engineers Inc., 2017.
 - [105] M. Ambroise, S. Buccelli, F. Grassia, A. Pirog, Y. Bornat, M. Chiappalone, and T. Levi, “Biomimetic neural network for modifying biological dynamics during hybrid experiments,” *Artif. Life Robot.*, vol. 22, no. 3, pp. 398–403, 2017.
 - [106] E. M. Izhikevich, “Simple model of spiking neurons,” *IEEE Transactions on neural networks*, vol. 14, no. 6, pp. 1569–1572, 2003.
 - [107] K. Akbarzadeh-Sherbaf, B. Abdoli, S. Safari, and A. H. Vahabie, “A scalable FPGA architecture for randomly connected networks of hodgkin-huxley neurons,” *Frontiers in Neuroscience*, vol. 12, no. OCT, 2018.
 - [108] A. Sripad, G. Sanchez, M. Zapata, V. Pirrone, T. Dorta, S. Cambria, A. Marti, K. Krishnamourthy, and J. Madrenas, “SNAVA—A real-time multi-FPGA multi-model spiking neural network simulation architecture,” *Neural Networks*, vol. 97, pp. 28–45, 2018.
 - [109] C. M. Zhang, G. C. Qiao, S. G. Hu, J. J. Wang, Z. W. Liu, Y. A. Liu, Q. Yu, and Y. Liu, “A versatile neuromorphic system based on simple neuron model,” *AIP Advances*, vol. 9, no. 1, 2019.

- [110] S. S. Guo, L. Wang, S. Q. Wang, Y. Deng, Z. J. Yang, S. M. Li, Z. G. Xie, Q. Dou, and M. Assoc Comp, "A Systolic SNN Inference Accelerator and its Co-optimized Software Framework," in *Glslvlsi '19 - Proceedings of the 2019 on Great Lakes Symposium on Vlsi*, Proceedings - Great Lakes Symposium on VLSI, pp. 63–68, 2019.
- [111] X. Huang, E. Jones, S. Zhang, S. Xie, S. Furber, Y. Goulermas, E. Marsden, I. Baistow, S. Mitra, and A. Hamilton, "Spiking neural network based low-power radioisotope identification using FPGA," Institute of Electrical and Electronics Engineers Inc., 2020.
- [112] S. B. Furber, F. Galluppi, S. Temple, and L. A. Plana, "The spinnaker project," *Proceedings of the IEEE*, vol. 102, no. 5, pp. 652–665, 2014. Publisher: IEEE.
- [113] B. Abdoli and S. Safari, "A reconfigurable real-time neuromorphic hardware for spiking winner-take-all network," *International Journal of Circuit Theory and Applications*, vol. 48, no. 12, pp. 2141–2152, 2020.
- [114] W. Guo, H. E. Yantir, M. E. Fouda, A. M. Eltawil, and K. N. Salama, "Towards efficient neuromorphic hardware: Unsupervised adaptive neuron pruning," *Electronics (Switzerland)*, vol. 9, no. 7, pp. 1–15, 2020.
- [115] M. Gholami, E. Zaman Farsa, and G. Karimi, "Reconfigurable field-programmable gate array-based on-chip learning neuromorphic digital implementation for nonlinear function approximation," *International Journal of Circuit Theory and Applications*, 2021.
- [116] H. Zheng, Y. Guo, X. Yang, S. Xiao, and Z. Yu, "Balancing the Cost and Performance Trade-offs in SNN Processors," *IEEE Transactions on Circuits and Systems II: Express Briefs*, pp. 1–1, 2021.
- [117] M. T. L. Aung, C. Qu, L. Yang, T. Luo, R. S. M. Goh, and W.-F. Wong, "DeepFire: Acceleration of Convolutional Spiking Neural Network on Modern Field Programmable Gate Arrays," in *2021 31st International Conference on Field-Programmable Logic and Applications (FPL)*, pp. 28–32, Aug. 2021.
- [118] J. J. Wu, Y. Zhan, Z. X. Peng, X. L. Ji, G. Y. Yu, R. Zhao, and C. Wang, "Efficient Design of Spiking Neural Network With STDP Learning Based on Fast CORDIC," *Ieee Transactions on Circuits and Systems I-Regular Papers*, vol. 68, no. 6, pp. 2522–2534, 2021.
- [119] A. H. Ali, M. Zain, S. M. Kazim, and M. Hasan, "Energy Efficient FPGA Implementation of a Spiking Neural Network," in *2022 IEEE 3rd Global Conference for Advancement in Technology (GCAT)*, pp. 1–6, Oct. 2022.
- [120] S. Hwang, Y. Hwang, D. Kim, J. Lee, H. K. Choe, J. Lee, H. Kang, and J. Kung, "ReplaceNet: real-time replacement of a biological neural circuit with a hardware-assisted spiking neural network," *Frontiers in Neuroscience*, vol. 17, 2023.
- [121] K. Kauth, T. Stadtmann, V. Sobhani, and T. Gemmeke, "neuroAIx-Framework: design of future neuroscience simulation systems exhibiting execution of the cortical microcircuit model 20× faster than biological real-time," *Frontiers in Computational Neuroscience*, vol. 17, 2023.
- [122] K. Wang, J. Wang, X. Hao, B. Deng, Z. Zhang, and G. Yi, "Large-Scale Bio-Inspired FPGA Models for Path Planning," *IEEE Transactions on Biomedical Circuits and Systems*, 2023.
- [123] R. Wang, J. Zhang, T. Wang, J. Liu, and G. Zhang, "A Resource-Efficient Scalable Spiking Neural Network Hardware Architecture with Reusable Modules and Memory Reutilization," *IEEE Transactions on Circuits and Systems II: Express Briefs*, 2023.
- [124] C. Shi, X. Fu, H. Wang, Y. Lin, Y. Jiang, L. Liu, N. Wu, and M. Tian, "Ghost Reservoir: A Memory-Efficient Low-Power and Real-Time Neuromorphic Processor of Liquid State Machine With On-Chip Learning," *IEEE Transactions on Circuits and Systems II: Express Briefs*, 2024.
- [125] Q. Chen, X. Dong, D. Ma, and X. Zhu, "A Hardware Accelerator of the Convolutional Spike Neural Network Based on STDP Online Learning," in *2024 Conference of Science and Technology for Integrated Circuits (CSTIC)*, pp. 1–3, IEEE, 2024.
- [126] W. Liu, S. Xiao, Y. Liu, and Z. Yu, "SC-PLR: An Approximate Spiking Neural Network Accelerator with On-Chip Predictive Learning Rule," *IEEE Transactions on Biomedical Circuits and Systems*, 2024.
- [127] M. Saponati and M. Vinck, "Sequence anticipation and spike-timing-dependent plasticity emerge from a predictive learning rule," *Nature Communications*, vol. 14, no. 1, p. 4985, 2023.
- [128] H. Hellmich and H. Klar, "An FPGA based simulation acceleration platform for spiking neural networks," in *The 2004 47th Midwest Symposium on Circuits and Systems, 2004. MWSCAS'04.*, vol. 2, pp. II–II, IEEE, 2004.

- [129] H. H. Hellmich, M. Geike, P. Griep, P. Mahr, M. Rafanelli, and H. Klar, "Emulation engine for spiking neurons and adaptive synaptic weights," vol. 5, pp. 3261–3266, 2005.
- [130] E. Ros, E. M. Ortigosa, R. Agís, R. Carrillo, and M. Arnold, "Real-time computing platform for spiking neurons (RT-spike)," *IEEE Transactions on Neural Networks*, vol. 17, no. 4, pp. 1050–1063, 2006.
- [131] B. Glackin, J. Harkin, T. M. McGinnity, L. P. Maguire, and Q. Wu, "Emulating spiking neural networks for edge detection on FPGA hardware," in *2009 International Conference on Field Programmable Logic and Applications*, pp. 670–673, IEEE, 2009.
- [132] S. F. Yang, Q. Wu, and R. F. Li, "A case for spiking neural network simulation based on configurable multiple-FPGA systems," *Cognitive Neurodynamics*, vol. 5, no. 3, pp. 301–309, 2011.
- [133] D. Neil and S. C. Liu, "Minitaur, an event-driven FPGA-based spiking network accelerator," *IEEE Transactions on Very Large Scale Integration (VLSI) Systems*, vol. 22, no. 12, pp. 2621–2628, 2014.
- [134] I. Kiselev, D. Neil, and S. Liu, "Event-driven deep neural network hardware system for sensor fusion," in *2016 IEEE International Symposium on Circuits and Systems (ISCAS)*, pp. 2495–2498, 2016.
- [135] R. M. Wang, C. S. Thakur, and A. van Schaik, "An FPGA-based massively parallel neuromorphic cortex simulator," *Frontiers in Neuroscience*, vol. 12, no. APR, 2018.
- [136] J. H. Han, Z. L. Li, W. M. Zheng, and Y. H. Zhang, "Hardware Implementation of Spiking Neural Networks on FPGA," *Tsinghua Science and Technology*, vol. 25, no. 4, pp. 479–486, 2020.
- [137] S. Li, Z. Zhang, R. Mao, J. Xiao, L. Chang, and J. Zhou, "A Fast and Energy-Efficient SNN Processor with Adaptive Clock/Event-Driven Computation Scheme and Online Learning," *IEEE Transactions on Circuits and Systems I: Regular Papers*, vol. 68, no. 4, pp. 1543–1552, 2021.
- [138] Y. Liu, Y. Chen, W. Ye, and Y. Gui, "FPGA-NHAP: A General FPGA-Based Neuromorphic Hardware Acceleration Platform With High Speed and Low Power," *IEEE Transactions on Circuits and Systems I: Regular Papers*, vol. 69, pp. 2553–2566, June 2022.
- [139] Y. Chen, W. Ye, Y. Liu, and H. Zhou, "SiBrain: A Sparse Spatio-Temporal Parallel Neuromorphic Architecture for Accelerating Spiking Convolution Neural Networks With Low Latency," *IEEE Transactions on Circuits and Systems I: Regular Papers*, 2024.
- [140] D. Roggen, S. Hofmann, Y. Thoma, and D. Floreano, "Hardware spiking neural network with run-time reconfigurable connectivity in an autonomous robot," vol. 2003-January, pp. 199–208, Institute of Electrical and Electronics Engineers Inc., 2003.
- [141] S. Bellis, K. M. Razeed, C. Saha, K. Delaney, C. O'Mathuna, A. Pounds-Cornish, G. De Souza, M. Colley, H. Hagaras, G. Clarke, V. Callaghan, C. Argyropoulos, C. Karistianos, and G. Nikiforidis, "FPGA implementation of spiking neural networks - An initial step towards building tangible collaborative autonomous agents," pp. 449–452, 2004.
- [142] A. Upegui, C. A. Peña-Reyes, and E. Sanchez, "An FPGA platform for on-line topology exploration of spiking neural networks," *Microprocessors and Microsystems*, vol. 29, no. 5, pp. 211–223, 2005.
- [143] R. Guerrero-Rivera, A. Morrison, M. Diesmann, and T. C. Pearce, "Programmable logic construction kits for hyper-real-time neuronal modeling," *Neural Computation*, vol. 18, no. 11, pp. 2651–2679, 2006.
- [144] R. Guerrero-Rivera and T. C. Pearce, "Attractor-based pattern classification in a spiking FPGA implementation of the olfactory bulb," in *2007 3rd International IEEE/EMBS Conference on Neural Engineering*, pp. 593–599, IEEE, 2007.
- [145] H. Shayani, P. J. Bentley, and A. M. Tyrrell, "An FPGA-based model suitable for evolution and development of spiking neural networks," pp. 197–202, 2008.
- [146] S. P. Johnston, G. Prasad, L. Maguire, and T. M. McGinnity, "An FPGA hardware/software co-design towards evolvable spiking neural networks for robotics application," *International Journal of Neural Systems*, vol. 20, no. 6, pp. 447–461, 2010.
- [147] F. Mondada, E. Franzi, and A. Guignard, "The development of khepera," in *Experiments with the mini-robot khepera, proceedings of the first international khepera workshop*, pp. 7–14, 1999.
- [148] L.-C. Caron, F. Mailhot, and J. Rouat, "FPGA implementation of a spiking neural network for pattern matching," in *2011 IEEE International Symposium of Circuits and Systems (ISCAS)*, pp. 649–652, IEEE, 2011.
- [149] J. L. RossellÓ, V. Canals, A. Morro, and A. Oliver, "Hardware implementation of stochastic spiking neural networks," *International Journal of Neural Systems*, vol. 22, no. 4, 2012.

- [150] T. Iakymchuk, A. Rosado, J. V. Frances, and M. Bataller, *Fast Spiking Neural Network architecture for low-cost FPGA devices*. 2012 7th International Workshop on Reconfigurable and Communication-Centric Systems-on-Chip, 2012.
- [151] B. Deng, M. Zhang, F. Su, J. Wang, X. Wei, and B. Shan, "The implementation of feedforward network on field programmable gate array," in *2014 7th International Conference on Biomedical Engineering and Informatics*, pp. 483–487, 2014.
- [152] Q. Wang, Y. Jin, and P. Li, "General-purpose LSM learning processor architecture and theoretically guided design space exploration," Institute of Electrical and Electronics Engineers Inc., 2015.
- [153] E. Z. Farsa, S. Nazari, and M. Gholami, "Function approximation by hardware spiking neural network," *Journal of Computational Electronics*, vol. 14, no. 3, pp. 707–716, 2015.
- [154] S. Gomar, M. Mirhassani, M. Ahmadi, and M. Seif, "A digital neuromorphic circuit for neural-glial interaction," vol. 2016-October, pp. 213–218, Institute of Electrical and Electronics Engineers Inc., 2016.
- [155] C. Lammie, T. Hamilton, M. R. Azghadi, and Ieee, "Unsupervised Character Recognition with a Simplified FPGA Neuromorphic System," in *2018 IEEE International Symposium on Circuits and Systems*, IEEE International Symposium on Circuits and Systems, 2018.
- [156] M. Heidarpur, A. Ahmadi, M. Ahmadi, and M. R. Azghadi, "CORDIC-SNN: On-FPGA STDP learning with izhikevich neurons," *IEEE Transactions on Circuits and Systems I: Regular Papers*, vol. 66, no. 7, pp. 2651–2661, 2019.
- [157] Z. B. Kuang, J. Wang, S. M. Yang, G. S. Yi, B. Deng, X. L. Wei, and Ieee, "Digital Implementation of the Spiking Neural Network and Its Digit Recognition," in *Proceedings of the 2019 31st Chinese Control and Decision Conference*, Chinese Control and Decision Conference, pp. 3621–3625, 2019.
- [158] H. Asgari, B. M. N. Maybodi, M. Payvand, and M. R. Azghadi, "Low-Energy and Fast Spiking Neural Network for Context-Dependent Learning on FPGA," *IEEE Transactions on Circuits and Systems II: Express Briefs*, vol. 67, no. 11, pp. 2697–2701, 2020.
- [159] M. Liang, J. Zhang, and H. Chen, "A 1.13uJ/Classification Spiking Neural Network Accelerator with a Single-Spike Neuron Model and Sparse Weights," in *2021 IEEE International Symposium on Circuits and Systems (ISCAS)*, pp. 1–5, 2021.
- [160] B. Deng, Y. Fan, J. Wang, and S. Yang, "Reconstruction of a Fully Paralleled Auditory Spiking Neural Network and FPGA Implementation," *IEEE Transactions on Biomedical Circuits and Systems*, vol. 15, pp. 1320–1331, Dec. 2021.
- [161] A. Heitmann, G. Psychou, G. Trensche, C. E. Cox, W. W. Wilcke, M. Diesmann, and T. G. Noll, "Simulating the Cortical Microcircuit Significantly Faster Than Real Time on the IBM INC-3000 Neural Supercomputer," *Frontiers in Neuroscience*, vol. 15, 2022.
- [162] S. Hu, T. Li, Y. Zuo, P. Zhou, R. Ma, and G. Qiao, "A Binarized Systolic Array-Based Neuromorphic Architecture with High Efficiency," in *2022 6th International Conference on Information Technology, Information Systems and Electrical Engineering (ICITISEE)*, pp. 595–599, Dec. 2022.
- [163] A. Carpegna, A. Savino, and S. Di Carlo, "Spiker+: a framework for the generation of efficient Spiking Neural Networks FPGA accelerators for inference at the edge," *IEEE Transactions on Emerging Topics in Computing*, 2024. Publisher: IEEE.
- [164] A. Carpegna, A. Savino, and S. Di Carlo, "Spiker: an FPGA-optimized Hardware accelerator for Spiking Neural Networks," in *2022 IEEE Computer Society Annual Symposium on VLSI (ISVLSI)*, pp. 14–19, July 2022.
- [165] D. E. Ipatov, A. V. Zverev, and Ieee, "Development of Neuromorphic Accelerator," in *2019 20th International Conference of Young Specialists on Micro/Nanotechnologies and Electron Devices*, International Conference and Seminar of Young Specialists on Micro-Nanotechnologies and Electron Devices, pp. 720–725, 2019.
- [166] S. Yang, J. Wang, X. Hao, H. Li, X. Wei, B. Deng, and K. A. Loparo, "BiCoSS: Toward Large-Scale Cognition Brain With Multigranular Neuromorphic Architecture," *IEEE Transactions on Neural Networks and Learning Systems*, 2021.
- [167] M. Pearson, I. Gilhespy, K. Gurney, C. Melhuish, B. Mitchinson, M. Nibouche, and A. Pipe, "A real-time, FPGA based, biologically plausible neural network processor," vol. 3697 LNCS, pp. 1021–1026, 2005.
- [168] O. Y. H. Cheung, P. H. W. Leong, E. K. C. Tsang, and B. E. Shi, "A Scalable FPGA Implementation

- of Cellular Neural Networks for Gabor-type Filtering,” in *The 2006 IEEE International Joint Conference on Neural Network Proceedings*, pp. 15–20, 2006.
- [169] K. Cheung, S. R. Schultz, and P. H. W. Leong, “A parallel spiking neural network simulator,” pp. 247–254, 2009.
- [170] C. H. Ang, C. Jin, P. H. Leong, and A. van Schaik, “Spiking neural network-based auto-associative memory using FPGA interconnect delays,” in *2011 International Conference on Field-Programmable Technology*, pp. 1–4, IEEE, 2011.
- [171] J. Luo, G. Coapes, P. Degenaar, T. Yamazaki, T. Mak, and C. Tin, “A real-time silicon cerebellum spiking neural model based on FPGA,” in *2014 International Symposium on Integrated Circuits (ISIC)*, pp. 276–279, 2014.
- [172] B. C. d. Vangel, C. Torres-Huitzil, and B. Girau, “Spiking dynamic neural fields architectures on FPGA,” in *2014 International Conference on ReConfigurable Computing and FPGAs (ReConFig14)*, pp. 1–6, 2014.
- [173] S.-i. Amari, “Dynamics of pattern formation in lateral-inhibition type neural fields,” *Biological cybernetics*, vol. 27, no. 2, pp. 77–87, 1977.
- [174] P. C. Holanda, C. R. W. Reinbrecht, G. Bontorin, V. V. Bandeira, and R. A. L. Reis, “DHANA: A NoC-based neural network hardware architecture,” in *2016 IEEE International Conference on Electronics, Circuits and Systems (ICECS)*, pp. 177–180, 2016.
- [175] J. Luo, G. Coapes, T. Mak, T. Yamazaki, C. Tin, and P. Degenaar, “Real-Time Simulation of Passage-of-Time Encoding in Cerebellum Using a Scalable FPGA-Based System,” *IEEE Transactions on Biomedical Circuits and Systems*, vol. 10, no. 3, pp. 742–753, 2016.
- [176] H. Lin, A. Zjajo, and R. v. Leuken, “Digital spiking neuron cells for real-time reconfigurable learning networks,” in *2017 30th IEEE International System-on-Chip Conference (SOCC)*, pp. 163–168, 2017.
- [177] S. Yang, J. Wang, B. Deng, C. Liu, H. Li, C. Fietkiewicz, and K. A. Loparo, “Real-time neuromorphic system for large-scale conductance-based spiking neural networks,” *IEEE Transactions on Cybernetics*, vol. 49, no. 7, pp. 2490–2503, 2019.
- [178] J. L. Zhang, H. Wu, J. S. Wei, S. J. Wei, H. Chen, and Ieee, *An Asynchronous Reconfigurable SNN Accelerator With Event-Driven Time Step Update*. 2019 Ieee Asian Solid-State Circuits Conference, 2019.
- [179] H. Fang, A. Shrestha, Z. Zhao, Y. Li, and Q. Qiu, “An event-driven neuromorphic system with biologically plausible temporal dynamics,” vol. 2019-November, Institute of Electrical and Electronics Engineers Inc., 2019.
- [180] H. Fang, Z. Mei, A. Shrestha, Z. Zhao, Y. Li, and Q. Qiu, “Encoding, model, and architecture: Systematic optimization for spiking neural network in FPGAs,” in *Proceedings of the 39th International Conference on Computer-Aided Design*, pp. 1–9, 2020.
- [181] J. P. Mitchell, C. D. Schuman, and T. E. Potok, “A Small, Low Cost Event-Driven Architecture for Spiking Neural Networks on FPGAs,” Association for Computing Machinery, 2020.
- [182] V. P. Nambiar, E. K. Koh, J. Pu, A. Mani, W. M. Ming, L. Fei, W. L. Goh, and A. T. Do, “Scalable Block-Based Spiking Neural Network Hardware with a Multiplierless Neuron Model,” in *2020 IEEE International Symposium on Circuits and Systems (ISCAS)*, pp. 1–5, 2020.
- [183] V. Sakellariou and V. Paliouras, “An FPGA Accelerator for Spiking Neural Network Simulation and Training,” in *2021 IEEE International Symposium on Circuits and Systems (ISCAS)*, pp. 1–5, 2021.
- [184] T. N. N. Nguyen, B. Veeravalli, and X. Fong, “Connection Pruning for Deep Spiking Neural Networks with On-Chip Learning,” in *ACM International Conference Proceeding Series*, 2021.
- [185] J. Mack, R. Purdy, K. Rockowitz, M. Inouye, E. Richter, S. Valancius, N. Kumbhare, M. S. Hassan, K. Fair, J. Mixter, and A. Akoglu, “RANC: Reconfigurable Architecture for Neuromorphic Computing,” *IEEE Transactions on Computer-Aided Design of Integrated Circuits and Systems*, vol. 40, pp. 2265–2278, Nov. 2021.
- [186] V. Truong-Tuan, C. Hoang-Phuong, A. Pham-Tuan, P. Pham-Hong, Q. H. Dang, H. Nguyen-Huy, and M. Nguyen-Duc, “FPGA Implementation of Parallel Neurosynaptic Cores for Neuromorphic Architectures,” in *2021 19th IEEE International New Circuits and Systems Conference (NEWCAS)*, pp. 1–4, 2021.
- [187] H. Wang, Z. He, T. Wang, J. He, X. Zhou, Y. Wang, L. Liu, N. Wu, M. Tian, and C. Shi,

- “TripleBrain: A Compact Neuromorphic Hardware Core With Fast On-Chip Self-Organizing and Reinforcement Spike-Timing Dependent Plasticity,” *IEEE Transactions on Biomedical Circuits and Systems*, vol. 16, pp. 636–650, Aug. 2022.
- [188] S. Zhao, J. Yang, J. Wang, C. Fang, T. Liu, S. Zhang, and M. Sawan, “A 0.99-to-4.38 uJ/class Event-Driven Hybrid Neural Network Processor for Full-Spectrum Neural Signal Analyses,” *IEEE Transactions on Biomedical Circuits and Systems*, vol. 17, pp. 598–609, June 2023.
- [189] J. N. Allen, H. S. Abdel-Aty-Zohdy, and R. L. Ewing, “Plasticity recurrent spiking neural networks for olfactory pattern recognition,” vol. 2005, pp. 1741–1744, 2005.
- [190] B. Girau and C. Torres-Huitzil, “FPGA implementation of an integrate-and-fire LEGION model for image segmentation,” in *ESANN*, pp. 173–178, 2006.
- [191] D. Wang and D. Terman, “Locally excitatory globally inhibitory oscillator networks,” *IEEE transactions on neural networks*, vol. 6, no. 1, pp. 283–286, 1995.
- [192] A. Cassidy, S. Denham, P. Kanold, A. Andreou, and Ieee, *FPGA based silicon spiking neural array*. 2007 Ieee Biomedical Circuits and Systems Conference, 2007.
- [193] S. Y. Bonabi, H. Asgharian, R. Bakhtiari, S. Safari, and M. N. Ahmadabadi, “FPGA implementation of a cortical network based on the Hodgkin-Huxley neuron model,” vol. 7663 LNCS, pp. 243–250, 2012.
- [194] M. E. Dean, C. D. Schuman, and J. D. Birdwell, “Dynamic adaptive neural network array,” vol. 8553 LNCS, pp. 129–141, Springer Verlag, 2014.
- [195] J. P. Mitchell, G. Bruer, M. E. Dean, J. S. Plank, G. S. Rose, and C. D. Schuman, “NeoN: Neuromorphic control for autonomous robotic navigation,” in *2017 IEEE International Symposium on Robotics and Intelligent Sensors (IRIS)*, pp. 136–142, 2017.
- [196] J. P. Mitchell, M. E. Dean, G. R. Bruer, J. S. Plank, and G. S. Rose, “DANNA 2: Dynamic adaptive neural network arrays,” Association for Computing Machinery, 2018.
- [197] T. Nanami and T. Kohno, “An FPGA-based cortical and thalamic silicon neuronal network,” *Journal of Robotics Networking and Artificial Life*, vol. 2, no. 4, pp. 238–242, 2016.
- [198] T. Kohno and K. Aihara, “Digital spiking silicon neuron: concept and behaviors in GJ-coupled network,” in *Proceedings of International Symposium on Artificial Life and Robotics*, vol. 2007, 2007.
- [199] P. Wilson, B. Metcalfe, J. Graham-Harper-Cater, and J. A. Bailey, “A reconfigurable architecture for real-time digital simulation of neurons,” in *2017 Intelligent Systems Conference (IntelliSys)*, pp. 66–75, 2017.
- [200] E. Z. Farsa, A. Ahmadi, M. A. Maleki, M. Gholami, and H. N. Rad, “A Low-Cost High-Speed Neuromorphic Hardware Based on Spiking Neural Network,” *IEEE Transactions on Circuits and Systems II: Express Briefs*, vol. 66, no. 9, pp. 1582–1586, 2019.
- [201] S. Gupta, A. Vyas, and G. Trivedi, “FPGA implementation of simplified spiking neural network,” Institute of Electrical and Electronics Engineers Inc., 2020.
- [202] B. U. V. Prashanth and M. R. Ahmed, “FPGA Implementation of Bio-inspired Computing Based Deep Learning Model,” in *Lecture Notes in Networks and Systems*, vol. 127, pp. 237–245, Springer, 2021.
- [203] Z. Wang, Y. Zhong, X. Cui, Y. Kuang, and Y. Wang, “A Spiking Neural Network Accelerator based on Ping-Pong Architecture with Sparse Spike and Weight,” in *2023 IEEE International Symposium on Circuits and Systems (ISCAS)*, pp. 1–5, May 2023.
- [204] F. Palumbo, C. Sau, D. Pani, P. Meloni, L. Raffo, and Ieee, “Feasibility study of real-time Spiking Neural Network simulations on a Swarm Intelligence based digital architecture,” in *2017 Ieee International Parallel and Distributed Processing Symposium Workshops*, IEEE International Symposium on Parallel and Distributed Processing Workshops, pp. 247–250, 2017.
- [205] D. Gerlinghoff, Z. Wang, X. Gu, R. S. Mong Goh, and T. Luo, “A Resource-efficient Spiking Neural Network Accelerator Supporting Emerging Neural Encoding,” in *2022 Design, Automation & Test in Europe Conference & Exhibition (DATE)*, pp. 92–95, Mar. 2022.
- [206] J. Kim, V. Kornijcuk, C. Ye, and D. S. Jeong, “Hardware-Efficient Emulation of Leaky Integrate-and-Fire Model Using Template-Scaling-Based Exponential Function Approximation,” *IEEE Transactions on Circuits and Systems I: Regular Papers*, vol. 68, pp. 350–362, Jan. 2021.
- [207] S. Gomar and M. Ahmadi, “Digital Realization of PSTDP and TSTD Learning,” vol. 2018-July, International Joint Conference on Neural Networks (IJCNN), 2018.

- [208] M. Nouri, M. Jalilian, M. Hayati, and D. Abbott, "A Digital Neuromorphic Realization of Pair-Based and Triplet-Based Spike-Timing-Dependent Synaptic Plasticity," *IEEE Transactions on Circuits and Systems II: Express Briefs*, vol. 65, no. 6, pp. 804–808, 2018.
- [209] B. U. Pedroni, S. Sheik, S. Joshi, G. Detorakis, S. Paul, C. Augustine, E. Neftci, and G. Cauwenberghs, "Forward table-based presynaptic event-triggered spike-timing-dependent plasticity," pp. 580–583, Institute of Electrical and Electronics Engineers Inc., 2016.
- [210] B. Belhadj, J. Tomas, O. Malot, G. N. Kaoua, Y. Bornat, and S. Renaud, "FPGA-based architecture for real-time synaptic plasticity computation," in *2008 15th IEEE International Conference on Electronics, Circuits and Systems*, pp. 93–96, 2008.
- [211] E. Jokar and H. Soleimani, "Digital Multiplierless Realization of a Calcium-Based Plasticity Model," *IEEE Transactions on Circuits and Systems II: Express Briefs*, vol. 64, no. 7, pp. 832–836, 2017.
- [212] T. S. Mak, G. Rachmuth, L. Kai Pui, and P. Chi-Sang, "Field Programmable Gate Array Implementation of Neuronal Ion Channel Dynamics," in *Conference Proceedings. 2nd International IEEE EMBS Conference on Neural Engineering, 2005.*, pp. 144–148, 2005.
- [213] P. Pourhaj and D. H. Y. Teng, "FPGA based pipelined architecture for action potential simulation in biological neural systems," 2010.
- [214] J. L. G. Peña, T. E. F. Carmona, M. A. A. Rodriguez, C. A. D. Rodriguez, and T. J. Borgonio, "Efficient FPGA Implementation of Circuits Based on Spiking Neural P Systems," in *2019 IEEE International Fall Meeting on Communications and Computing (ROC&C)*, pp. 51–54, 2019.
- [215] T. Levi, F. Khoiratee, S. Saighi, and Y. Ikeuchi, "Digital implementation of Hodgkin-Huxley neuron model for neurological diseases studies," *Artificial Life and Robotics*, vol. 23, no. 1, pp. 10–14, 2018.
- [216] S. Y. Bonabi, H. Asgharian, S. Safari, and M. N. Ahmadabadi, "FPGA implementation of a biological neural network based on the hodgkin-huxley neuron model," *Frontiers in Neuroscience*, vol. 8, no. Nov, 2014.
- [217] F. Grassia, T. Kohno, and T. Levi, "Digital hardware implementation of a stochastic two-dimensional neuron model," *Journal of Physiology Paris*, vol. 110, no. 4, pp. 409–416, 2016.
- [218] M. Heidarpour, A. Ahmadi, and R. Rashidzadeh, "A CORDIC Based Digital Hardware for Adaptive Exponential Integrate and Fire Neuron," *IEEE Transactions on Circuits and Systems I: Regular Papers*, vol. 63, no. 11, pp. 1986–1996, 2016.
- [219] S. Gomar and A. Ahmadi, "Digital multiplierless implementation of biological adaptive-exponential neuron model," *IEEE Transactions on Circuits and Systems I: Regular Papers*, vol. 61, no. 4, pp. 1206–1219, 2014.
- [220] M. Heidarpur, A. Ahmadi, and N. Kandalafi, "A digital implementation of 2D Hindmarsh-Rose neuron," *Nonlinear Dynamics*, vol. 89, no. 3, pp. 2259–2272, 2017.
- [221] M. Hayati, M. Nouri, D. Abbott, and S. Haghiri, "Digital Multiplierless Realization of Two-Coupled Biological Hindmarsh-Rose Neuron Model," *IEEE Transactions on Circuits and Systems II: Express Briefs*, vol. 63, no. 5, pp. 463–467, 2016.
- [222] A. Kazemi, A. Ahmadi, and S. Gomar, "A digital synthesis of hindmarsh-rose neuron: A thalamic neuron model of the brain," pp. 238–241, Institute of Electrical and Electronics Engineers Inc., 2014.
- [223] M. Hayati, M. Nouri, S. Haghiri, and D. Abbott, "Digital Multiplierless Realization of Two Coupled Biological Morris-Lecar Neuron Model," *IEEE Transactions on Circuits and Systems I: Regular Papers*, vol. 62, no. 7, pp. 1805–1814, 2015.
- [224] J. Pu, W. L. Goh, V. P. Nambiar, Y. S. Chong, and A. T. Do, "A Low-Cost High-Throughput Digital Design of Biorealistic Spiking Neuron," *IEEE Transactions on Circuits and Systems II: Express Briefs*, vol. 68, pp. 1398–1402, Apr. 2021.
- [225] S. Haghiri, A. Zahedi, A. Naderi, and A. Ahmadi, "Multiplierless Implementation of Noisy Izhikevich Neuron with Low-Cost Digital Design," *IEEE Transactions on Biomedical Circuits and Systems*, vol. 12, no. 6, pp. 1422–1430, 2018.
- [226] M. A. Imani, A. Ahmadi, M. Radmalekshahi, and S. Haghiri, "Digital Multiplierless Realization of Coupled Wilson Neuron Model," *IEEE Transactions on Biomedical Circuits and Systems*, vol. 12, no. 6, pp. 1431–1439, 2018.
- [227] E. Rahimian, S. Zabihi, M. Amiri, and B. Linares-Barranco, "Digital Implementation of the

- Two-Compartmental Pinsky-Rinzel Pyramidal Neuron Model,” *IEEE Transactions on Biomedical Circuits and Systems*, vol. 12, no. 1, pp. 47–57, 2018.
- [228] H. Soleimani and E. M. Drakakis, “An Efficient and Reconfigurable Synchronous Neuron Model,” *Ieee Transactions on Circuits and Systems li-Express Briefs*, vol. 65, no. 1, pp. 91–95, 2018.
 - [229] J. Zhang, J. Wang, X. Hao, and N. Zhang, “Neural Network with Cascaded Model Dendritic morphologic and FPGA Implementation,” in *2022 41st Chinese Control Conference (CCC)*, pp. 7088–7093, July 2022.
 - [230] D. Kudithipudi, C. Schuman, C. M. Vineyard, T. Pandit, C. Merkel, R. Kubendran, J. B. Aimone, G. Orchard, C. Mayr, R. Benosman, and others, “Neuromorphic computing at scale,” *Nature*, vol. 637, no. 8047, pp. 801–812, 2025. Publisher: Nature Publishing Group UK London.
 - [231] IEEE International Roadmap for Devices and Systems, “Executive summary 2022,” 2022.